



NATIONAL TECHNICAL UNIVERSITY OF ATHENS
SCHOOL OF MECHANICAL ENGINEERING
FLUIDS SECTION
PARALLEL CFD & OPTIMIZATION UNIT

Optimization of Vehicle Air Duct Geometry

Diploma Thesis

Marianna Panagiotidou

Supervision:

Professor K. C. Giannakoglou

Athens
February 2019

Optimization of Vehicle Air Duct Geometry

Diploma Thesis Abstract

Marianna Panagiotidou

The objective of this diploma thesis is to use a stochastic optimization method and implement it (constrained where needed) to optimize the shape of the defroster duct of a passenger car in order to achieve the fastest possible windshield defrosting and/or defogging. The optimal geometry can be used as a starting point for further optimization using the adjoint method in order to find the global optimum geometry. Furthermore, the effect of the duct width is studied in order to find an appropriate geometry in the case of a Head-Up Display (HUD) installation in the car.

The optimization process is based on a metamodel-assisted evolutionary algorithm (MAEA). The EASY platform developed by the Parallel CFD & Optimization Unit of the National Technical University of Athens (PCOpt/NTUA) is used. An additional tool developed by PCOpt/NTUA and used in this study is the regression model tool. This study is the sequel to a relevant diploma thesis (that of L. Germanou) in which the optimization problem of the defrosting performance was addressed exclusively by using the continuous adjoint method and an experiment was carried out to validate the results.

To achieve its objective, this diploma thesis incorporates design of experiments techniques, mesh morphing, regression models and evolutionary algorithms. The above have been decided in order to eliminate the dependency on the initialization of gradient-based optimization methods as well as the limited geometry morphing capacity which characterizes free-form deformation (FFD), due to fixed topology.

A new objective function that is more representative of the target of increasing the defrosting efficiency, being therefore more suitable for our study, is formulated and used. In order to address the problem, it is necessary to compute the percentage of the windshield area where the velocity is lower than a minimum acceptable value for sufficient defogging and defrosting. A step function, which assigns a zero penalty to cells with a velocity above the target value and a penalty of unity elsewhere, is adopted as the evaluation tool during the MAEA optimization. However, in order to be compatible with the next optimization step, which relies upon the continuous adjoint method, it is a prerequisite to express the performance of the duct with a differentiable function. For this purpose, a sigmoidal objective function is developed and two velocity thresholds are defined, a minimum acceptable value below which

maximum penalty is assigned and a target value above which no penalty is imposed. The min-max nature of the problem can be approximated satisfactorily by setting appropriate thresholds based on the requirements of the problem and the engineers' experience.

With this study, a new optimal geometry for the original width case was determined. This geometry has the same total pressure drop and a better velocity pattern, compared to the original one. It can be fed into the adjoint optimization method as a starting point in order to optimize geometry. Furthermore, the preliminary optimization steps for the reduced width duct gave the appropriate geometry for further optimization with stochastic and deterministic methods.

Major part of this diploma thesis was carried out in the premises of Toyota Motor Europe, in Belgium, with Mr. Antoine Delacroix as industrial advisor.

Βελτιστοποίηση Γεωμετρίας Αεραγωγού Αυτοκινήτου

Περίληψη Διπλωματικής Εργασίας

Μαριάννα Παναγιωτίδου

Σκοπός αυτής της διπλωματικής εργασίας είναι η χρήση μιας στοχαστικής μεθόδου και η εφαρμογή της (με τους κατάλληλους περιορισμούς) για τη βελτιστοποίηση του σχήματος του αεραγωγού ενός επιβατικού αυτοκινήτου ώστε να επιτευχθεί η ταχύτερη αποπάγωση/αποθάμβωση του ανεμοθώρακα (παρμπρίζ). Η βέλτιστη γεωμετρία μπορεί να χρησιμοποιηθεί ως σημείο εκκίνησης της συζυγούς μεθόδου προκειμένου να βρεθεί η ολικά βέλτιστη γεωμετρία. Επιπλέον, μελετάται η επίδραση του πλάτους του αγωγού προκειμένου να βρεθεί μια κατάλληλη γεωμετρία για την περίπτωση εγκατάστασης συστήματος διαφανούς οθόνης δεδομένων στο παρμπρίζ (Head-Up Display, HUD) στο αυτοκίνητο.

Η διαδικασία βελτιστοποίησης βασίζεται σε έναν εξελικτικό αλγόριθμο με μεταπρότυπα (ΜΑΕΑ). Χρησιμοποιείται η πλατφόρμα EASY που αναπτύχθηκε από τη Μονάδα Παράλληλης Υπολογιστικής Ρευστοδυναμικής & Βελτιστοποίησης του ΕΜΠ (ΜΠΥΡΒ/ΕΜΠ). Ένα επιπλέον εργαλείο που αναπτύχθηκε από τη ΜΠΥΡΒ/ΕΜΠ και χρησιμοποιήθηκε σε αυτή τη μελέτη είναι το εργαλείο μοντέλου παλινδρόμησης. Αυτή η μελέτη είναι η συνέχεια μιας σχετικής διπλωματικής εργασίας (της Λ. Γερμανού) στην οποία το πρόβλημα βελτιστοποίησης της απόδοσης αποπάγωσης εξετάστηκε αποκλειστικά με τη συζυγή μέθοδο και διεξήχθη ένα πείραμα για την επικύρωση των αποτελεσμάτων.

Αυτή η διπλωματική εργασία ενσωματώνει σχεδιασμό τεχνικών πειραμάτων, μορφοποίηση πλέγματος, μοντέλα παλινδρόμησης και εξελκτικούς αλγορίθμους. Τα παραπάνω επιλέχθηκαν προκειμένου να εξαλειφθεί η εξάρτηση από την αρχικοποίηση των μεθόδων βελτιστοποίησης με βάση την κλίση καθώς και η ικανότητα μορφοποίησης περιορισμένης γεωμετρίας, λόγω της σταθερής τοπολογίας ως αποτέλεσμα της μείωσης της ποιότητας λόγω της ευαισθησίας του πλέγματος.

Αναπτύχθηκε μια νέα αντικειμενική συνάρτηση που είναι πιο αντιπροσωπευτική του στόχου της αύξησης της αποπάγωσης και επομένως, περισσότερο κατάλληλη για την υπόψη μελέτη. Προκειμένου να αντιμετωπιστεί το πρόβλημα, είναι απαραίτητο να υπολογιστεί το ποσοστό της περιοχής του ανεμοθώρακα όπου η ταχύτητα είναι χαμηλότερη μιας ελάχιστης αποδεκτής τιμής για επαρκή αποθάμβωση και αποπάγωση. Υιοθετείται μια βηματική

συνάρτηση, η οποία αποδίδει μηδενική κύρωση σε κελιά με ταχύτητα πάνω από την τιμή-στόχο και ενιαία ποινή οπουδήποτε αλλού, ως εργαλείο αξιολόγησης κατά τη διάρκεια της βελτιστοποίησης μέσω εξελικτικών αλγορίθμων. Ωστόσο, για να είναι συμβατή με το επόμενο βήμα βελτιστοποίησης, της συζυγούς μεθόδου, είναι αναγκαίο να εκφραστεί με μια διαφορίσιμη συνάρτηση. Για το σκοπό αυτό, χρησιμοποιείται μια σιγμοειδής συνάρτηση και καθορίζονται δύο όρια ταχύτητας, μια ελάχιστη αποδεκτή τιμή κάτω από την οποία αποδίδεται η μέγιστη ποινή και μια τιμή-στόχος πάνω από την οποία αποδίδεται μηδενική ποινή. Η φύση ελαχιστοποίησης του προβλήματος μπορεί να προσεγγιστεί ικανοποιητικά με τον καθορισμό κατάλληλων κατωτάτων ορίων βάσει των απαιτήσεων του προβλήματος και της εμπειρίας.

Με αυτή τη μελέτη, προσδιορίστηκε μια νέα βέλτιστη γεωμετρία για την αρχική περίπτωση πλάτους. Αυτή η γεωμετρία έχει την ίδια πτώση πίεσης και ένα καλύτερο μοτίβο ταχύτητας, σε σύγκριση με το αρχικό. Μπορεί να τροφοδοτήσει τη μέθοδο βελτιστοποίησης με τη συζυγή τεχνική ως σημείο εκκίνησης για να βρει την ολικά βέλτιστη γεωμετρία. Επιπλέον, τα προκαταρκτικά βήματα βελτιστοποίησης για τον αγωγό μειωμένου πλάτους έδωσαν την κατάλληλη γεωμετρία για περαιτέρω βελτιστοποίηση με στοχαστικές και αιτιοκρατικές μεθόδους.

Μεγάλο τμήμα της διπλωματικής εργασίας εκπονήθηκε στις εγκαταστάσεις της Toyota Motor Europe, στο Βέλγιο, υπό την επίβλεψη του μηχανικού κ. A. Delacroix.

Acknowledgements

I am grateful to all the people who supported me during my occupation with my diploma thesis and throughout my studies in NTUA. First of all, I would like to express my profound gratitude to Prof. K. C. Giannakoglou, for trusting me with this very interesting and innovative project. His advice and corrections were valuable and I thank him for transmitting his knowledge and passion for his field of expertise all these years.

A great part of this diploma thesis, was realised in the premises of Toyota Motor Europe, in the department of 'Vehicle Performance Engineering'. Taking this opportunity, I would like to thank Mr. A. Delacroix, my industrial advisor, N. Yokoyama and M. Honda, my managers, for his persistence and guidance throughout this endeavour. I wholeheartedly thank especially Mr. A. Delacroix for his enthusiasm all these months and for sharing with me his knowledge and experience concerning the automotive industry.

I would also like to express my gratitude to Dr. K. Gkagkas for all his support in this venture.

In addition, I would like to express my deepest appreciation to all the members of the Parallel CFD & Optimization Unit of National Technical University of Athens for their help throughout my studies. Particularly, I wish to express my sincere thanks to Dr. V. Asouti, D. Kapsoulis and Dr. E. Papoutsis-Kiachagias for their continuous support and help during this project.

Last but not least, I would like to express my deepest gratitude to my professors and to all those who supported me throughout my studies. Their contribution has been invaluable and most appreciated.

Table of Contents

1	Introduction	1
1.1	HVAC – Defroster Nozzle	1
1.2	Head-Up Display.....	1
1.3	CFD-based Optimization	2
1.3.1	Optimization	3
1.3.2	Design of Experiments.....	4
1.3.3	Gradient-free Optimization.....	6
1.3.4	Gradient-based Optimization.....	7
1.4	Purpose and Structure of Thesis.....	7
2	Design of Experiments (DoE)	9
2.1	General.....	9
2.2	Factorial Design.....	9
2.2.1	Full Factorial Design.....	9
2.2.2	2 ⁿ Factorial Design	10
2.2.3	Full Factorial Design of 3 or more Levels.....	12
2.2.4	Complex full factorial design of many levels.....	13
2.3	Fractional Factorial.....	13
2.4	Central Composite Design	14
2.5	Other Types of Design	15
2.5.1	Block Design	15
2.5.2	Taguchi method.....	15
2.5.3	Box-Behnken	16
2.5.4	Optimal design.....	16
3	Evolutionary Algorithms	17
3.1	General.....	17
3.2	(μ,λ) Evolutionary Algorithm	17
3.3	EASY Software.....	19
3.4	Metamodel Assisted Evolutionary Algorithms (MAEA)	19
3.4.1	Off-line and On-line MAEA.....	20
3.4.2	MAEA with Low-Cost Pre-Evaluation	20
3.5	Regression Model.....	21
4	Optimization of the Original HVAC Duct	25
4.1	General.....	25
4.2	Design Parameters	25
4.3	Design Constraints	26
4.3.1	Geometric Constraints.....	26
4.3.2	Total pressure Drop.....	27
4.4	Sampling of Design Space	27
4.5	Preparation of New Geometries.....	28
4.5.1	CAD.....	29
4.5.2	Morphing.....	29
4.6	Solver & Mesh.....	32
4.7	Target & Objective Function.....	35
4.8	Results of DoE Study.....	38

4.9	EASY Loop.....	44
4.10	Results of the Optimization Loop	45
4.11	Study of Optimized Duct Performance	46
5	Study of Width Parameter	48
5.1	Explanation of Width Parameter	48
5.1.1	Parameters	48
5.1.2	Morphing.....	49
5.1.3	Results.....	49
5.2	Objective Function.....	51
5.2.1	Definition of Objective Function	51
5.2.2	Error of Objective Function	53
5.3	Results of Study	54
5.4	Operation for different mass flows	57
6	Conclusions and Future Research.....	59
6.1	Conclusions	59
6.2	Future Research	59
	Bibliography.....	60

1 Introduction

1.1 HVAC - Defroster Nozzle

HVAC units and distribution systems are an integral part of the cabin climate control function. To ensure the comfort of the occupants, i.e. drivers and the passengers, the right amount of conditioned air at desirable temperature and humidity levels should be delivered to the target locations (Park & Kim 2003, Sugarman 2005). Adequate flow delivery is also important for the safe operation of a vehicle that requires proper defogging and defrosting capabilities.

At the same time, the energy required for the flow delivery should be minimized for better fuel economy, while the adverse effects of the associated acoustic noises should be limited (Shojaeefard et al. 2015). To achieve these goals, the designs of the ducts and the registers as part of climate control system are carefully evaluated and optimized for greatly varying ambient conditions as part of vehicle development process.

Furthermore, due to the tight packaging in vehicle interiors, the available physical space for HVAC units and distribution systems is very limited. Designers of climate control systems are often required to work around the geometrical restrictions imposed by other vehicle interior components, often without up-front understanding of the impact of potential design changes on the system performance.

In addition, complex physics such as flow turbulence, thermal mixing and radiation play important roles in determining air flow distribution, fan power requirement, and air temperature stratification inside a vehicle cabin. However visualization and measurement of such physical effects are difficult in real vehicle applications.

System optimization in a climatic wind tunnel or through road testing for widely varying ambient conditions requires significant time and effort, particularly when some of the testing has to be conducted for transient conditions. Besides, the evaluation matrix tends to be large due to various operating modes (defrosting/ventilation/bi-level/foot well) of an HVAC system.

1.2 Head-Up Display

Inside the car cabin, installations can be found which interact with the HVAC air flow. Such an installation is the Head-up displays (HUDs). Head-up

displays are the current state-of-the-art solution to reducing driver errors originating from distractive interfaces, such as on-board entertainment displays or in-vehicle information systems (IVIS). Compared to head-down displays (HDDs) which are integrated into the vehicle's control panel, the frequency and duration of glances towards the display are reduced by presenting information directly on the windshield in the driver's field of vision (Ablassmeier et al., 2007). Consequently, the response time to unanticipated road events is reduced when information is displayed on a HUD instead of a HDD (Horrey and Wickens, 2004, Liu and Wen, 2004, Sojourner and Antin, 1990), and the number of collisions is significantly reduced (Charissis et al., 2008). Using HUDs also leads to a, generally, more consistent speed control and reduced mental workload (Liu and Wen, 2004), reduced navigational errors (Burnett, 2003), and smaller variances in lateral accelerations and steering wheel angle (Yung-Ching, 2003).

Head-up displays can be divided in two categories: a) in-car and b) on-board.

In-car HUD displays are the most advanced form of HUDs. They provide the information on the windshield of the car and no external device is needed. The technology for HUD varies on the system. Some cars use transparent phosphors on the windshield that reacts when a laser shines on it. Only when the laser is on, is the information projected on the glass. Others use a similar system but incorporate mirrors to project the images on the windshield. A display unit is installed below the dashboard which projects the information on a set of mirrors. The driver actually sees is the virtual image of the display screen in front of the windshield at a distance called the projection distance.

On-board HUD is a device which can be mounted on the top of the dashboard and projects information on its integrated transparent display. Instead of displaying the image on the windshield as the In-car HUD does, it projects the image on its own transparent screen. Most on-board HUDs work by linking to either driver phone's internal GPS or finding a signal of their own from a satellite to determine the velocity of the car at any given time, and display the information back on their display.

1.3 CFD-based Optimization

As proven, the accurate prediction of HVAC air flow and its interaction with cabin parts, is a mandatory process in order to design an HVAC system that works in the desired way.

Improving the performance of products, processes and services without increasing the cost has always been a major topic of interest for the engineering sector/industry. Optimization targets of engineering problems usually take the form of improvement of efficiency and/or reduction of/decrease in costs. For example, in the automotive industry, engineers try to optimize the shape of the vehicles to reduce drag and fuel consumption.

Computational Fluid Dynamics (CFD) has proven to be a valuable tool for predicting duct performances (pressure losses and relevant flow features) both in early and advanced phases of design. In internal aerodynamics, the aerodynamic CFD-based design optimization of ducts systems (e.g. HVAC system, cooling systems) has acquired an important role in the automotive industry. CFD-based optimization is implemented to enhance the efficiency of the HVAC system by achieving improved defrosting and defogging performance of the vehicle. Since their introduction in automotive applications, shape and topology optimization have been gradually gaining more ground and are now considered as established approaches to complex optimization problems.

Over the years several approaches to the methods of optimization have been studied and implemented. It is at the engineer's discretion to select the appropriate optimization method that will yield the optimal results with the least required effort and cost. Irrespective of the optimization method, in order to proceed it is necessary to first model the optimization process which includes identifying the problem, setting an objective and defining the design variables and constraints, if any, under which the problem will be studied. In shape optimization, the parameterization of the geometry is also a key issue to address. By parameterizing the geometry, a number of control points are defined and the optimization process will search for the optimal solution for the sum/total of the control points.

Thus, an optimization process that incorporates a CFD tool for air flow prediction can result to an optimal HVAC design.

1.3.1 Optimization

Optimization methods have been implemented in order to solve quantifiable problems of several scientific fields, such as mechanics, physics, and economics. The problems to be solved can have one single target (Single Objective Optimization – SOO) or many targets (Multi-objective optimization – MOO). The purpose of an optimization method is to specify the values of the free parameters/variables of the problem that will yield a minimum or maximum value of the objective function defined by the requirements of the problem (minimization or maximization problems). In this diploma thesis, only minimization problems are presented, however, this does not limit the scope of the work since maximization problems can easily be transformed to minimization ones. The free parameters are named design variables. It is common to have equality and inequality constraints that have to be respected in order to reach an acceptable final solution.

In CFD-based optimization, it is very common to have contradictory objectives. A problem of more than one targets can be addressed as a multi-objective optimization (MOO) or, alternatively, can be transformed to a single objective optimization (SOO) by incorporating all the objectives into a weighted

one. Based on the nature of the problem and the available resources, any of the two options can be selected.

Optimization methods are distinguished based on the way they seek for the optimal solution. Stochastic methods explore the design space in a randomized way whereas deterministic methods will reach the optimal solution by taking into consideration the gradient of the objective function. Nowadays, new hybrid methods that combine elements of the two methods have been developed. In complex aerodynamic problems, developing a deterministic method requires more time and effort and the developed method cannot always be adapted to similar problems. On the other hand, the deterministic method will converge to an optimal solution in significantly less cycles than a stochastic method; however, based on the initialization of the method, this optimum might not be the global optimum of the problem. Stochastic methods are comparatively more general and more appropriate for use in several problems of the same nature. One of the main drawbacks of stochastic methods is that they can be very slow in reaching the optimal solution, which will however be the global optimum of the design space. The latter is secured if instead of improving a single candidate solution, as is the case in deterministic methods, several candidate solutions are evaluated and monitored. As a trade-off to the improved performance of the method, population-based optimization methods have a higher computational cost than single-individual based methods.

Thus, in a given problem which has independent design variables that their values affect the output variables, it is better to study this relation among these variables prior to an extensive optimization process.

1.3.2 Design of Experiments

The Experiment Design or Design of Experiments (DoE) is an efficient and ubiquitous process for planning experiments and exploring complex problems (Antony 2003). It is widely used in research and development as an effective tool to develop and improve existing products and processes. Implementing a DoE will yield the relationship between factors affecting a process and the output of that process (cause & effect relationships).

As an alternative to the DoE approach, the one-factor-at-a-time (OFAT) and trial-and-error practices can be applied; however, these do not guarantee lower cost or accurate and complete results. Altering one factor at a time in studies has the drawback of higher costs since more experiments need to be carried out. Moreover, in real life problems where more than one factors can change at a time and the output is dependent on combinations of factors in addition to single factor changes, the OFAT approach cannot capture the complexity of the problem. On the other hand, trial and error practices require a deep understanding of the problem and can be very slow and not lead to the optimal results.

A design of experiments can be used to choose between alternatives (comparative experiment), identify the key factors affecting the output (screening experiment) or model the response surface of the problem. The latter is adopted when the objective is to reach a target, maximize or minimize a response, reduce variations in the process, make a process robust or optimize based on multiple goals. Once the objective of the study is determined, the next step of the Design of Experiments is to identify and select the process model. The process model consists of the inputs and outputs of the problem. The inputs of the process can be controlled or not and are called factors and co-factors respectively. Defining the range of the factors should not be done light-heartedly since extreme values can result in unfeasible runs and reduced smoothness in the response surface. The output of the experiment, the response, is studied as a function of the above factors.

An important part of the DoE is to select the experimental design, i.e. the way in which the design space will be sampled. The amount of information obtained by a DoE for a given amount of experiment cost can be maximized by selecting the appropriate experiment design. Based on the number of factors and the objective of the study, a randomized or structured/systematic design can be selected. Randomized designs are the method of choice in comparative studies, whereas in screening and response surface studies systematic designs yield better results. Standardized designs include the full factorial design in which all possible combinations of the factor levels are selected to run, or fractional factorial design which consists of only an adequately chosen fraction of the full factorial design.

As stated previously, one of the functions of the DoE study is to use the experimental data to derive an approximation of the cause and effect relationship by linking the inputs and outputs of the problem. Not only does the DoE unveil the direct link between a single factor and the response but it also deals with the interactions, i.e. the situation in which the simultaneous influence of the input variables on the response is not additive. The Design of Experiments along with Regression analysis will generate a mathematical model which describes the model process.

The mathematical model relates the dependent variables (responses) to a function of the independent variables (factors) and the unknown coefficients of the function. The most known form of regression analysis is the least-squares method. In order to perform a regression analysis, it is necessary to have at least as many sets of experimental data as the number of coefficients of the regression model. Regression analysis can be used for both interpolation and extrapolation, however, the latter can be very susceptible to errors since it is making assumptions on data outside the range of the available data and the difference between estimation and actual data can be significant.

1.3.3 Gradient-free Optimization

One of the main representatives of stochastic optimization methods (gradient-free optimization methods) are the evolutionary algorithms (Giannakoglou, 2002, Marco and Lanteri, 2000). These stochastic methods are inspired by Charles Darwin's theory of evolution, according to which the individuals of a population will compete with each other in order to procure the necessary resources to survive and attract partners to reproduce. Certain individuals that are fitter or adapt quicker to the challenges of their environment have a better chance of succeeding in surviving and reproducing, therefore, it is the genes of this set of individuals that will be passed on to the next generations. This concept is known as natural selection and it entails that the individuals of future generations will carry the best characteristics from the previous generations. In this way, as the generations progress, the populations evolve and adapt to the current environment. In a similar way, the evolutionary algorithm will spawn a population of candidate solutions which will be evaluated in order to select the elite population, most of which will reproduce to create the new generations of offspring. The offspring candidate solutions might perform better than the parents. By evaluating the offspring, selected individuals are selected to become the parents of the next generation and the cycle continues until one of the terminating criteria is met. Four basic operators are employed in the optimization method; a selection operator to select the parent population, a crossover operator to generate the offspring based on the combination of the parents' genes, a mutation operator to introduce new genetic material to the population and an elitism operator to select the individuals that will consist the elite population.

Evolutionary algorithms were first introduced in the 1960's but at the time the lack of computational resources rendered them unfeasible. It wasn't until the 1990, when computer science was advanced enough and computers were more affordable, that evolutionary algorithms were established as an effective optimization method.

The most known applications of evolutionary algorithms are the genetic algorithms, the evolution strategies and genetic programming. In all three applications some distinctive traits can be identified. Evolutionary algorithms monitor populations of individuals that evolve throughout the generations. Being a population-based optimization method, the evolutionary algorithm will converge to the global optimum of the problem, therefore increasing the reliability of the method but the computational cost as well. In order to determine the successful individuals that will comprise the parents of the next generation it is necessary to evaluate their performance by assigning scores based on the objective function of the problem. These ratings can be cost scores in minimization problems or fitness scores in maximization problems. In evolutionary algorithms, the evolution of the populations is based on the fitness scores of the individuals. Moving a generation forward entails that new

individuals, offspring of the fittest parents, will be introduced to the population whereas the weakest individuals of the previous generation will be eliminated. Finally, the succession of generations is characterized by heredity from the parents to the offspring, but new traits can also be spawned in a stochastic way.

Evolutionary algorithms are well established methods thanks to the simplicity of their implementation as long as the necessary software is available. In order to implement an evolutionary algorithm to a new problem, it is not necessary to tamper with the optimization process as is the case in deterministic optimization where the formulation of the problem changes with every new objective function. The evaluation tool, necessary to assign fitness scores to the candidate solutions, is external and treated as a black box, hence, simplifying the setup of the optimization process.

1.3.4 Gradient-based Optimization

A gradient-based method is an algorithm to solve optimization problems with the search directions defined by the gradient of the objective function at the current point. One major representative of the gradient-based optimization methods is the adjoint method. The adjoint results to computational tools for the computation of the gradient of the (objective) function while simultaneously ensuring that the basic equations defining the problem are satisfied (in aerodynamics flow equations: Euler or Navier-Stokes equations). The term adjoint and the relevant expressions were first introduced in control theory. In mathematics, the equivalent subject is that of Lagrange multipliers. Bearing in mind that in an optimization method, the gradient of the objective function is required in order to point to the solution that yields the minimum value of the objective function (e.g. though the steepest descend method), it is common practice when referring to adjoint methods in aerodynamics to incorporate both the computation of the gradient and the minimization process of the objective function, i.e. the wholesome of the optimization problem or of inverse design.

1.4 Purpose and Structure of Thesis

From all the above, it can be concluded that the correct design of the HVAC unit plays a major role in the car industry. Furthermore, in cases where a new car design is primarily based on a previous model, the design optimization of the HVAC unit is mandatory.

The objective of this diploma thesis is to use Design of Experiment and stochastic CFD optimization methods to optimize the shape of the defroster duct of a passenger car (TOYOTA Yaris) in order to achieve the fastest possible windshield defrosting and/or defogging. Furthermore, a preliminary optimization is carried out taking into account the use of a HUD display which limits the available area for the HVAC defroster nozzle.

The stochastic optimization process is based on a metamodel-assisted evolutionary algorithm (MAEA) which is materialized by the EASY platform developed by the PCOpt/NTUA while incorporating regression models. The candidate designs that come of are further optimized using EASY and CFD tools.

This study is the sequel to a relevant diploma thesis (that of L. Germanou) in which the optimization problem of the defrosting performance was addressed exclusively using the continuous adjoint method and an experiment was carried out to validate the results. This thesis aims to establish a procedure in which optimized candidate solutions are derived from stochastic optimization process and can subjectively be used as the starting point of the costly CFD –adjoint optimization process to achieve the global minimum of the cost function.

This thesis consists of 7 chapters. In Chapter 2, the Design of Experiments (DoE) methods are discussed while in Chapter 3 the Evolutionary Algorithm is presented. The optimization of an existing HVAC duct is presented in Chapter 4. In Chapter 5 the effect of the limited width duct due to the HUD display is assessed and a preliminary procedure of finding the optimized duct geometry which can further be fed into an EA or adjoint optimization method is carried out. Finding the optimal geometry is out of this thesis scope, since the exact HUD display geometry is not available. Finally, in Chapter 6, the outcome of this work is concluded and some proposals for further steps are provided.

2 Design of Experiments (DoE)

2.1 General

In its simplest form of DoE, studies and experiments are carried out with only one free variable. The scientist alters the value of the variable in every run of the experiment and observes the impact on the outcome of the experiment. However, nowadays it is very common to have many design variables, therefore in this case the scientist has to alter the value of the variables one by one and then carry out the experiment. There is, however, a more efficient method in carrying out the experiments. Instead of altering the variables one at a time, the scientist can alter all the design variables simultaneously. The advantages are:

1. The experiment will take place fewer times, therefore the cost and time required is reduced.
2. The complexity of reality is delineated. In the physical world, problems have various variables that change simultaneously.
3. Information on the impact of the outcome by the alteration of a combination of free variables is made available.

Design of Experiments defines the way the variable values will be altered in order to ensure that the execution of the experiments yield useful data for analysis. Design methods are described in the paragraphs below.

2.2 Factorial Design

2.2.1 Full Factorial Design

Full Factorial Design requires the highest number of runs of the computation compared to other types of design for the same level of discretization of the design space (Antony 2003). In this case, for k design variables, each discretized in l_i levels of same distances between the two limits, the number of experiments required is the product $l_1 l_2 \dots l_k$. For instance, for three design variables A,B,C with four (4), three (3), and two (2) levels respectively per variable, $4 \times 3 \times 2 = 24$ experiments are required in a full factorial design. The matrix of this design is presented below:

0	0	0
1	0	0
2	0	0
3	0	0
0	1	0
1	1	0
2	1	0
3	1	0

0	2	0
1	2	0
2	2	0
3	2	0
0	0	1
1	0	1
2	0	1
3	0	1

0	1	1
1	1	1
2	1	1
3	1	1
0	2	1
1	2	1
2	2	1
3	2	1

Every triplet of values defines univocally one (computational) experiment. In the third column, the values (0,1,2,3) correspond to the four same-distance levels of the variable C. Therefore, 0 is the lowest level and 3 is the highest level of the variable, as defined by the user. In the second column, the values (0,1,2) are the 3 levels of variable B, etc.

More often than not, the number and runtime of the computational experiment reach large prohibitive levels in a full factorial design since all possible combinations of the design variables need to be examined. In this type of design, the responses for all possible combinations will be computed if the design variables are discrete and all the levels of the variables are considered. In the case of continuous variables, the accuracy of the design relies on the discretization applied and the number of levels examined. Most of the problems in mechanics comprise continuous variables, as is the case in this diploma thesis. Further examples of this design with limited variables and levels are presented.

2.2.2 2ⁿ Factorial Design

This type of full factorial design is the simplest possible form and takes into consideration only the upper and lower limits of the design variables (Antony 2003). This type of design is preferred in problems with qualitative variables as well as in cases where a quick review of the responses is needed. In a problem of two free variables A and B, each of which has two levels, the possible combinations according to the 2ⁿ factorial design are: 00, 01, 11, 10. If the real values of the respective levels of the variables are a_1, a_2 and b_1, b_2 then the possible combinations can also be expressed as $(a_1b_1, a_1b_2, a_2b_1, a_2b_2)$. The results of the problem solved for the combinations of variables is symbolized as $f(\cdot)$, where the contents of the parenthesis are the levels of the variables. Therefore, the proposed experiments yields the responses $f(a_1b_1), f(a_1b_2), f(a_2b_1)$ and $f(a_2b_2)$. This design is called 2ⁿ symmetric. Since only two levels are examined, it is common practice to represent the two levels as - and + that correspond to 0 and 1. According to the introduced notation, the matrix of the full design is:

Factors	
A	B
-	-
-	+
+	-
+	+

The following equations are solved in order to specify the main effect of the variables A and B:

$$F_A = \frac{1}{2} [(f(a_2b_1) - f(a_1b_1)) + (f(a_2b_2) - f(a_1b_2))] \quad 2.1$$

$$F_B = \frac{1}{2} [(f(b_2a_1) - f(b_1a_1)) + (f(b_2a_2) - f(b_1a_2))]$$

where F denotes the main effect

Four experiments are required in order to specify the main effects of the design variables. The main effect indicates how much, or not, does the variable impact the result of the experiment.

In experiments with stochasticity, each experiment is carried out p times in order to define the best sample. The results are added and the mean value is calculated and subsequently used in equation 2.1 for the calculation of the main effects. In this case, equations 2.1 are expressed as:

$$F_A = \frac{\sum_{i=1}^p (f_i(a_2b_1) - f_i(a_1b_1))}{2p} + \frac{\sum_{i=1}^p (f_i(a_2b_2) - f_i(a_1b_2))}{2p} \quad 2.2$$

$$F_B = \frac{\sum_{i=1}^p (f_i(b_2a_1) - f_i(b_1a_1))}{2p} + \frac{\sum_{i=1}^p (f_i(b_2a_2) - f_i(b_1a_2))}{2p}$$

This thesis does not address stochastic experiments; however, the above paragraph is presented for the sake of completeness.

The interaction AB is defined as the mean value of the difference of the effect variable B has when variable A is at level 1 (its value being a_2) and the effect variable B has when variable A is at level 0 (its value being a_1):

$$F_{AB} = \frac{f(a_2b_2) + f(a_1b_1)}{2} - \frac{f(a_2b_1) + f(a_1b_2)}{2} \quad 2.3$$

where F denotes the effect of the interaction. It is proven that the same equation applies for the interaction BA.

In general, the method described above can also be implemented for problems of k free variables, in which case the design is called 2^k symmetric. The

total number of main effects is k , the interaction of the two factors is $\binom{k}{2}$, the interactions of three factors are $\binom{k}{3}$ and so on. It is recalled that:

$$\binom{k}{i} = \frac{k!}{i!(k-i)!} \quad 2.4$$

The total number of effects is $2^k - 1$. The property of binomial factors $\sum_{i=1}^k \binom{k}{i} = 2^k - 2$ indicates that the addition of the effect of a constant factor results in a total number of effects of $2^k - 1$. The effect of the constant factor includes all the effects that are not examined and considered constant. The term "effects" denotes the sum of main effects and interactions. For instance, in a problem of 4 design variables ($k = 4$), the 2^4 factorial design has the following effects:

$$F_0, F_a, F_b, F_{ab}, F_c, F_{ac}, F_{bc}, F_{abc}, F_d, F_{ad}, F_{bd}, F_{abd}, F_{acd}, F_{cd}, F_{bcd}, F_{abcd}$$

The effect F_0 indicates the effect of the constant factor which is created by the variables that are not examined. In a way, it does not fall into the category of effects since it does not include any of the examined variables.

It must be mentioned that in stochastic experiments, each experiment is carried out n times and statistical analysis of the findings takes place afterwards. Stochastic experiments are outside the scope of this diploma thesis, therefore, further analysis is not deemed necessary.

2.2.3 Full Factorial Design of 3 or more Levels

It is a fact that in industrial applications variables are quite frequently separated in two levels in order to proceed with a quick study and obtain an estimation of the space of the responses with the least possible computational effort and cost (Antony 2003). A study of more levels is required when the desired level of accuracy is high and therefore the approximation of the real response map with a regression surface of higher order is attempted.

The example of an experiment of k free design variables of three levels will be presented. The aforementioned design requires 3^k experiments, all of which have to be carried out in order for the factorial design to be full, with $3^k - 1$ effects. The number of runs of the experiments increases exponentially with the increase of number of free variables. For instance, for a problem of three variables $3^3 = 27$ runs are required, whereas when the number of variables increases to 5, the required number of experiments reaches $3^5 = 243$, therefore increasing significantly the total runtime and cost of the design.

The main effects of the variables are k . The interactions are of 2,3, ..., k factors. The need of an approximation model of higher order results in the increase of the order of the interactions. Interactions of the $AB^{C_2}C^{C_3} \dots K^{C_k}$ form

appear now, where c_i are integers that point to the power of the respective variable in the particular interaction. For example, the interactions of a problem of 4 design variables are:

$$ABCD, ABCD^2, ABC^2D, AB^2CD, ABC^2D^2, AB^2C^2D, AB^2CD^2, AB^2C^2D^2$$

In this thesis it is decided that interactions where the power of the first variable is more than one will be ignored. These interactions are useful when designing a block (a type of design that will not be presented in this diploma thesis), a fractional factorial design and approximation models. These interactions correspond to nothing in the physical world. The interactions to be analyzed are selected by the user based on their experience and the nature and requirements of the problem. A main criterion for this selection is the importance of the variables in each interaction, the desired accuracy of the study as well as the cost of executing the experiments (high cost can result in reduced capacity for experiments leading to reduced study of the interactions).

2.2.4 Complex full factorial design of many levels

So far only symmetric designs have been presented, i.e. design where the variables are discretized in the same number of levels. However, in several cases designs that require combination of variables of different number of levels are utilized. These designs are called non-symmetric designs. In a non-symmetric design with several and different levels of the variables, the matrix of the design variable vectors is significantly more complex and attention, while devising the experiments, is needed to ensure all possible combinations of the variables are studied. This method is not used in this diploma thesis and therefore will not further be presented.

2.3 Fractional Factorial

Fractional designs are expressed using the notation l^{k-p} , where l is the number of levels of each factor investigated, k is the number of factors investigated, and p describes the size of the fraction of the full factorial used (Antony 2003). Formally, p is the number of generators, assignments as to which effects or interactions are confounded, i.e., cannot be estimated independently of each other. A design with p such generators is a $1/(l^p)$ fraction of the full factorial design.

For example, a 2^{5-2} design is $1/4$ of a two level, five factor factorial design. Rather than the 32 runs that would be required for the full 2^5 factorial experiment, this experiment requires only eight runs.

2.4 Central Composite Design

The central composite design is a design of experiments that results in great accuracy of the model that will be trained later without increasing though the number of levels of the variables. It is applied only in problems with quantitative design variables that are continuous in the design space. This design consists of:

- A factorial design, full or fractional. In full factorial designs of a small number of levels, Central Composite Design can be implemented to ensure increased accuracy of the design. This design is called initial design.
- A group of central points, whose values are the mean value of the products of the variables and a factor. For further explaining, visualize the problem of three design variables where the CCD would place the central points at the center of the squares of the design space.
- A group of axial points, whose values are determined by the central points, increasing by one factor the respective variable at a time.

In the case of two levels per variable, the central points are calculated as the mean value of the levels of each variable. Each coordinate of the central points is multiplied by a factor to produce the axial points. This factor is the radius of the circle formulated by the axial points with respect to the central points (i.e. the axial points are located on a circle in relation to the central points). It is an important parameter of this type of design and its value changes based on the problem at hand and the approximation area. In a 2^p factorial design, for a radius greater than one, the values of the axial points in each direction denote the new minima and maxima of each variable. It is noted that the radius is defined non-dimensionally in relation to the values of the design variables.

There are three distinct types of designs:

1. Circumscribed (CCC): This is the most common type of design. The distance from the center to the axial points is defined based on the problem and which points of the design space are of greater interest. The axial points expand the limits of each variable. There is a cyclical, spherical, hyper-spherical symmetry depending on the variables. The circumscribed design is produced by the existing factorial design augmented with axial and central points.
2. Inscribed (CCI): The initial limits of the variables are not violated. The axial points serve as the limits of the variables and a factorial design is produced in the interior. The distinction from other types of design is the fact that the factorial design is not based on the limits of the variables. It is, essentially, a circumscribed design divided by an appropriate number in order to detain the design to the limits of the

variables. It is therefore a product of a scaling of the above mentioned type of design.

3. Face Centered (CCF): In this type of design the axial points are located in the middle of each edge of the squares of the factorial design space. The radius of the central composite design is equal to one.

These types of designs are rotational. The selection of the radius is an important feature when devising the design. In order to maintain their rotational properties, the radius depends on the number of runs of the experiment and the design variables: $a = [\text{number of factorial runs}]^{1/4}$

For instance, in a full factorial design of k design variables with two levels per radius, the radius is calculated as: $a = [2^k]^{1/4}$

The axial points are located at a distance $+a$, $-a$ respectively in relation to the central point and the (active) variable whose value is altered. For a radius of one, the axial points reside on the limits of the variables.

2.5 Other Types of Design

2.5.1 Block Design

In combinatorial mathematics, a block design is a set together with a family of subsets (repeated subsets are allowed at times) whose members are chosen to satisfy some set of properties that are deemed useful for a particular application (Cavazzuti 2013). These applications come from many areas, including experimental design, finite geometry, software testing, cryptography, and algebraic geometry. Many variations have been examined, but the most intensely studied are the balanced incomplete block designs (BIBDs or 2-designs) which historically were related to statistical issues in the experiments. A block design in which all the blocks have the same size is called uniform.

2.5.2 Taguchi method

Taguchi's designs aimed to allow greater understanding of variation than did many of the traditional designs from the analysis of variance (Cavazzuti 2013). Taguchi contended that conventional sampling is inadequate here as there is no way of obtaining a random sample of future conditions. Taguchi proposed extending each experiment with an "outer array" (possibly an orthogonal array); the "outer array" should simulate the random environment in which the product would function. This is an example of judgmental sampling.

Later innovations in outer arrays resulted in "compounded noise." This involves combining a few noise factors to create two levels in the outer array: First, noise factors that drive output lower, and second, noise factors that drive

output higher. "Compounded noise" simulates the extremes of noise variation but uses fewer experimental runs than would previous Taguchi designs.

2.5.3 Box-Behnken

Box–Behnken designs are experimental designs for response surface methodology (Cavazzuti 2013), devised by George E. P. Box and Donald Behnken in 1960, to achieve the following goals:

- Each factor, or independent variable, is placed at one of three equally spaced values, usually coded as $-1, 0, +1$.
- The design should be sufficient to fit a quadratic model, that is, one containing squared terms, products of two factors, linear terms and an intercept.
- The ratio of the number of experimental points to the number of coefficients in the quadratic model should be reasonable.
- The estimation variance should more or less depend only on the distance from the center and should not vary too much inside the smallest (hyper) cube containing the experimental points.

Each design can be thought of as a combination of a two-level (full or fractional) factorial design with an incomplete block design. In each block, a certain number of factors are put through all combinations for the factorial design, while the other factors are kept at the central values. For instance, the Box–Behnken design for 3 factors involves three blocks, in each of which 2 factors are varied through the 4 possible combinations of high and low. It is necessary to include center points as well (in which all factors are at their central values)

2.5.4 Optimal design

In the design of experiments, optimal designs are a class of experimental designs that are optimal with respect to some statistical criterion. The creation of this field of statistics has been credited to Danish statistician Kirstine Smith.

In the design of experiments for estimating statistical models, optimal designs allow parameters to be estimated without bias and with minimum variance. A non-optimal design requires a greater number of experimental runs to estimate the parameters with the same precision as an optimal design. In practical terms, optimal experiments can reduce the costs of experimentation.

The optimality of a design depends on the statistical model and is assessed with respect to a statistical criterion, which is related to the variance-matrix of the estimator. Specifying an appropriate model and specifying a suitable criterion function both require understanding of statistical theory and practical knowledge with designing experiments.

3 Evolutionary Algorithms

3.1 *General*

As mentioned previously, the stochastic optimization process in this thesis is based on a metamodel-assisted evolutionary algorithm (MAEA) which is materialized by EASY platform developed by the PCOpt/NTUA while incorporating regression models. In the paragraphs below, EA, EASY, MAEA and regression models are described.

3.2 *(μ,λ) Evolutionary Algorithm*

The (μ,λ) Evolutionary Algorithm makes use of three populations, the parent population P_{μ}^g , the offspring population P_{λ}^g and the elite population P_e^g of every generation (g). The parent population comprises of the individuals that will reproduce to generate the offspring of the next generation (Giannakoglou 2005). The elite populations comprises of the fittest/best individuals (solutions) that have emerged from the very beginning of the evolution procedure until the current generation. The elite population is used to reinforce the “good”/desired characteristics of the individuals of the new generation (elitism) and provides the optimal solutions at any point of the evolution procedure/at the point that the evolutionary procedure is stopped.

The process of an Evolutionary Algorithm is described in the following steps:

1. Initialization: The population of the zero generation ($g = 0$) is initialized by a Pseudo Random Number Generator. The generator will provide each individual of the population with a value for each of the design variables in a random manner. The values of the design variables have to satisfy the limits/have to lie in the design space set by the user. The user can opt for specified/preset values for the zero generation.
2. Evaluation: All the individuals of the offspring population P_{λ}^g are evaluated on the appropriate evaluation tool, i.e. the selected evaluation tool is called for each vector of design variables and the vectors of the objective functions values and of the constraints, if applicable, are obtained. In the case of constrained problems, the vector of constraints is added to the objective function vector. The use of penalization functions is

required in order to deal with in-equality constraints of the following form $c_k(\vec{x}) \leq c_k^{thres}$. Depending on the severity/magnitude of the violation of the constraints, a penalty (most frequently, exponential) penalization is added to the objective function vector. This penalty takes the form of $exp\left(a_k \frac{c_k(x) - c_k^{thres}}{d_k^* - c_k^{thres}}\right)$ where a_k is the coefficient that shows/expresses how severe the penalty will be, $c_k(x)$ is the value of the constraint for the respective variable vector, c_k^{thres} is the maximum allowed value of the constraint, d_k^* is the relaxation boundary that defines the value after which death penalty will be assigned/implemented to the variable vector. The death penalty is a penalty so high that, when added to the objective function vector, the candidate solution will no longer participate in the reproductive procedure/process in a significant manner.

3. Renewal of the elite population: The elite population P_e^g is renewed with the individuals of the new generation that have better characteristics/performance. Each individual of the population is compared to the individuals of the elite population. If there is a design variable vector that is superior in at least one objective and not inferior in any of the objectives, then this design variable vector is included in the elite population by replacing the worst/weakest elite individual.
4. Elitism: Elite individuals replace randomly some of the individuals of the offspring population. It is common practice to replace weak individuals in order to ensure that in the next generation there will be no worse solutions compared to the previous generation. This process is called Elitism.
5. Selection of parents: Making use of the parent selection operator will yield the next parent generation. Both the offspring population of the current generation and the parent population of the previous generation participate in the procedure of selection.
6. Reproduction: The process of reproduction will yield the next generation of offspring. Two or more parents are selected and subsequently crossed over and mutated in order to generate a new offspring.
7. Convergence Criteria: The termination criteria, i.e. if the number of evaluations has reached a maximum level or if the process has converged and can no longer yield improved solutions compared to the current ones for a reasonable number of latest generations. If the stopping criteria are met the process terminates, if not it is resumed from step 2 with the offspring of the new.

3.3 EASY Software

Evolutionary Algorithm optimization can be carried out with several commercial or open-source software. In this diploma thesis, the EASY (Evolutionary Algorithm System) platform developed by the PCOpt/NTUA is used (Kampolis & Giannakoglou 2009). This platform is an optimization software designed for general purpose. As long as the evaluation tool is available, the EASY software can solve problems of any scientific field, single or multi objective, constrained or not. It is a powerful optimization tool already used by Industry.

The software incorporates both stochastic and deterministic methods that contribute, combined or separately, to the solution of each problem. In addition to the evaluation tool, the EASY software can also make use of low-cost metamodels for the evaluation of the fitness of the individuals. The metamodels employed are connected to the evolution and provide a low-cost estimation of the performance of each candidate solution. In this way, significant reduction of the computational complexity/cost can be achieved, due to the fact that fewer evaluations with the (most of the times) time-consuming evaluation tool are required. Another feature that allows further reduction of the computational cost and the runtime is the parallel evaluations of the fitness scores in CPUs and GPUs.

3.4 Metamodel Assisted Evolutionary Algorithms (MAEA)

In the majority of the problems where the appropriate-relative evaluation tool is time-consuming, such as solving the Navier-Stokes equations, the computational cost is prohibitively high, rendering thus the optimization process through EAs unfeasible. The use of metamodels contributes to the reduction of the number of evaluations and consequently the reduction of the computational time (Kampolis et al. 2007). Metamodels do not provide an exact evaluation of each individual but rather an approximation of the real vector of objectives with fractional computational resources. In the course of the evolution, the metamodel's role is to point to the most promising individuals that will be re-examined through the exact evaluation software. This technique is called Low-Cost Pre-Evaluation of the candidate solutions. The incorporation of metamodels in optimization through Evolutionary algorithms led to what is called today Metamodel Assisted Evolutionary Algorithms (Karakassis and Giannakoglou, 2006).

Metamodels have to be trained properly using points that have been already evaluated through the exact evaluation tool. The Database (DB) consists of variable vectors that have been evaluated by the exact evaluation tool. A subset of the database serves as the samples that will train the metamodel (training patterns); this subset is selected according to the type of the metamodel. The size of the subset is of great importance for the validity of the

metamodel; a non-representative sample may lead to false estimations of the variable vectors that are pre-examined.

The metamodels can be local or global. Local surrogate models approximate solutions of a defined area of the design space whereas global models provide reliable solutions for candidates in any area of the design space. Metamodels are also categorized based on their connectivity to the evolution, on-line or off-line.

3.4.1 Off-line and On-line MAEA

Off-line metamodels are usually global surrogate models. The metamodel is trained once before the initiation of the EA, therefore it is independent to the evolution of the solutions during the optimization. The exact evaluation software is used to create the database out of which samples will be selected automatically for the training of the metamodel. In multi objective optimization problems separate metamodels are trained for each objective function. In the course of the optimization process, only the approximation of the objective variable vector, provided by the pre-trained metamodel, is taken into consideration. Upon convergence of the optimization process the optimal design variable vector will be re-evaluated through the exact evaluation tool in order to specify the real objective variable vector.

On-line metamodels are surrogate models that are trained in the course of the optimization process. Initially the metamodel is trained by a training sample provided by the exact evaluation tool. Afterwards, as the generations evolve and additional exact evaluations have been made, the metamodel is re-trained by the renewed training sample. In the case of On-line MAEA, the evaluation tool and the metamodel are used alternatively. In this category of MAEA, the metamodel changes and adapts as the generations progress. Main representative of either category are the artificial neural networks.

3.4.2 MAEA with Low-Cost Pre-Evaluation

The Low-Cost Pre-Evaluation serves as a low-cost classifier of the design variable vectors of each generation (Kampolis, 2009, Giotis, 2001). The individuals with the most promising performance according to the metamodel approximation will be re-evaluated through the exact evaluation software. Experience shows that local metamodels provide more accurate approximations when the objective function space is complicated.

The steps of the MAEA that relies upon the Low-Cost Pre-Evaluation are presented below:

1. The optimization process begins with a conventional (μ, λ) EA, that is, the first generations are evaluated through the exact evaluation tool provided

by the user. The individuals of these first generations will be recorded in the database that will be later used for the training of the metamodel.

2. The training of the metamodel can take place only after the size of the database reaches a sufficient/adequate level. The fitness scores of the candidate solutions of the following generations will be approximated by the metamodel. The runtime and computational cost of the metamodel “evaluation” is insignificant compared to the exact evaluation. In local metamodels, the performance assigned to the candidate solution is site-specific, i.e. depends on the nearest points of the database and their performance.
3. The objective variable vectors that are acquired by the evaluation of each generation are ranked from most to least suitable. In single objective optimization this is an easy, univocal and self-evident/obvious task. On the contrary, in multi objective optimization, the comparison and classification is a much more complicated procedure. In the latter, the metamodel will yield one performance at a time.
4. The most promising candidate solutions of each generation are re-evaluated through the exact evaluation software. The number of these evaluations, implicitly determined by the user, defines the computational cost for each generation. The exact solutions enrich the database to be used for the training of the metamodel in next generations.
5. Each design variable vector is paired with its objective variable vector. The termination criteria check takes place, if the process has converged then the optimization process stops, if not the new generation is created and the process goes on.

3.5 Regression Model

Metamodels frequently used alongside Evolutionary Algorithms are the Artificial Neural Networks and Regression Models (Rao 2008). In this diploma thesis, offline Regression models were used therefore only these will be presented.

Regression analysis dates back to the 19th century when the need to determine the orbits of celestial bodies around the sun from astronomical observations was first addressed by Legendre and Gauss. The earliest form of regression is the well-known method of least squares in which a solution is approximated for overdetermined systems, i.e. systems where the number of equations is greater than the number of unknowns. The most important application of the method of least squares is the least square fitting, a mathematical procedure for determining the best fitting curve to a given set of points by minimizing the sum of the squares of the offsets of the points from the curve.

Regression analysis includes the dependent variable, the set of independent variables and the unknown coefficients of the function. A regression model will relate the dependent variable to a function of the independent variables and the unknown coefficients.

Based on the number of independent variables, regression analysis can be distinguished to single or multiple regression. In single regression, the effect of only one variable of the response is considered whereas in multiple regression several factors can enter the analysis separately so that the effect of each can be estimated.

Furthermore, regression models can be distinguished in two main categories, linear and nonlinear regression. In linear regression, the dependent variable is approximated by a linear combination of the independent variables. Linear regression consists of least squares fitting of lines as well as polynomials. On the other hand, nonlinear regression, such as exponential, logarithmic, trigonometric models, involves nonlinear combinations of the input factors. In nonlinear regression, there is no unique formula to determine the best fit function, therefore iterative methods and numerical optimization are implemented to determine the curve of global minima of error. In some cases, it is possible to linearise the approximation function and proceed with linear regression, however, this may entail severe implications to the model in terms of alterations in the error structure and effect of independent variables on the response.

Several key assumptions are made in order to implement a regression model, for instance homoscedasticity (constant variance) of the errors, normality of the error distribution, statistical independence of the errors and a representative sample of the population used for to train the regression model. Linear independence of the independent variables is a common assumption that however does not apply always, for example data fitting with polynomials is considered a linear regression model that treats the exponents as independent variables that are linearly dependent. Additional assumptions are made based on whether the regression is single or multiple and linear or non-linear.

Regression models can serve as a complimentary tool to evolutionary algorithms.

In Regression model, unknown parameters are introduced and the definition of them determines the quality of the adjustment of the polynomial function to the solutions of the real model. These parameters are computed by solving a simple linear method of least squares.

For a vector of N independent variables x , the first-order regression model is:

$$\hat{y}(\vec{x}) = b_0 + \sum_{n=1}^N b_n x_n + \varepsilon \quad 3.1$$

where b_n , $n = 0, \dots, N$ are the unknown parameters of the model and ε is the error.

The second-order regression model is defined in a similar way:

$$\hat{y}(\vec{x}) = b_0 + \sum_{n=1}^N b_n x_n + \sum_{i=1}^N b_{ii} x_i^2 + \sum_{i=1}^N \sum_{j=i+1}^N b_{ij} x_i x_j + \varepsilon \quad 3.2$$

where b_{ij} are the additional unknown parameters of the model.

The product of the design variables $x_i x_j$ reveals the interaction of the variables and constitutes a very important feature in complex problems with interactions. The above-mentioned models are the most frequently used, however, any other model of higher degree and different interactions can be devised and used. The order and interactions of variables of the model are subject to the nature of the problem and their definition depends on the knowledge and experience of the user.

Unknown parameters b_i of the regression model are defined by employing the Least Squares Method that minimizes the error ε . The assumption that K fitness scores y_1, y_2, \dots, y_k for the design variable vectors $\vec{x}_1, \vec{x}_2, \dots, \vec{x}_k$ are known is made. Both the objective variable vector y_i and the respective design variable vector x_{ij} are known, where i denotes the solution and j the respective design variable. Let ε_i be the error of the result of the least squares method to the real result, for the i observation. The analysis of a first-order regression models is presented for simplicity's sake. Utilizing a first-order model and solving for the error the following equation for each performance is obtained:

$$\varepsilon_i = y_i - b_0 - \sum_{j=1}^N b_j x_{ij} \quad 3.3$$

The Least Squares function is:

$$L = \sum_{i=1}^K \varepsilon^2 = \sum_{i=1}^K \left(y_i - b_0 - \sum_{j=1}^N b_j x_{ij} \right)^2 \quad 3.4$$

The function L has to be minimized with respect to the parameters b_j , therefore its first-order derivatives with respect to the parameters have to be zero:

$$\frac{\partial L}{\partial b_j} = -2 \sum_{i=1}^K \left(y_i - b_0 - \sum_{j=1}^N b_j x_{ij} \right) x_{ij} = 0 \quad j = 1, 2, \dots, k \quad 3.5$$

These equations can easily be solved when expressed in matrix form.
The initial equation of the observations is:

$$\mathbf{y} = \mathbf{X}\mathbf{b} + \boldsymbol{\varepsilon} \quad 3.6$$

$$\text{where } \mathbf{y} = \begin{bmatrix} y_1 \\ y_2 \\ \vdots \\ y_K \end{bmatrix}, \mathbf{X} = \begin{bmatrix} 1 & x_{11} & x_{12} & \dots & x_{1N} \\ 1 & x_{21} & x_{22} & \dots & x_{2N} \\ \vdots & \vdots & \vdots & \ddots & \vdots \\ 1 & x_{K1} & x_{K2} & \dots & x_{KN} \end{bmatrix}, \mathbf{b} = \begin{bmatrix} b_1 \\ b_2 \\ \vdots \\ b_N \end{bmatrix}, \boldsymbol{\varepsilon} = \begin{bmatrix} \varepsilon_1 \\ \varepsilon_2 \\ \vdots \\ \varepsilon_K \end{bmatrix}$$

In general, \mathbf{y} is a vector of dimension K , as long as the experiments, \mathbf{X} , are a matrix of dimensions $K \times N$ with N free variables, \mathbf{b} is a vector of dimension N and $\boldsymbol{\varepsilon}$ is a vector of K random errors.

The function L is expressed as:

$$L = \sum_{i=1}^K \varepsilon_i^2 = \boldsymbol{\varepsilon}'\boldsymbol{\varepsilon} = (\mathbf{y} - \mathbf{X}\mathbf{b})'(\mathbf{y} - \mathbf{X}\mathbf{b}) = \mathbf{y}'\mathbf{y} - 2\mathbf{b}'\mathbf{X}'\mathbf{y} + \mathbf{b}'\mathbf{X}'\mathbf{X}\mathbf{b} \quad 3.7$$

The symbol $(\cdot)'$ symbolizes the transposed matrix. By differentiating the above function in a similar manner as above, we get:

$$\begin{aligned} \frac{\partial L}{\partial \mathbf{b}} &= -2\mathbf{X}'\mathbf{y} + 2\mathbf{X}'\mathbf{X}\mathbf{b} = 0 \\ \mathbf{X}'\mathbf{X}\mathbf{b} &= \mathbf{X}'\mathbf{y} \end{aligned} \quad 3.8$$

The latter equation is identical to equation 3.5. Therefore the calculation of the elements of vector \mathbf{b} will take place through equation 3.8 in its matrix form.

$$\mathbf{b} = (\mathbf{X}'\mathbf{X})^{-1}\mathbf{X}'\mathbf{y} \quad 3.9$$

The matrix $\mathbf{X}'\mathbf{X}$ is of dimension $N \times N$ whereas $\mathbf{X}'\mathbf{y}$ is a vector of dimension N . Both are calculated relatively easy. The system can be solved by employing several methods, such as the Gauss Elimination. Since $\mathbf{X}'\mathbf{X}$ is a symmetrical matrix, the most straightforward way to solve is the Cholesky method.

After solving, the regression model can be expressed in the form of matrices:

$$\hat{\mathbf{y}}_i = \mathbf{X}\hat{\mathbf{b}} \quad 3.10$$

where $\hat{\mathbf{y}}_i$ is the prediction of the model for each vector $\hat{\mathbf{b}}$.

4 Optimization of the Original HVAC Duct

4.1 *General*

Scope of this work is the optimization of TOYOTA Yaris HVAC duct in order to achieve better performance with respect to the defrosting/defogging procedure.

4.2 *Design Parameters*

In order to proceed with shape optimization of the duct geometry, it is necessary to define first the design parameters and their range.

In the studied case, three design parameters which define the geometry are chosen, namely: 1) Distance: distance of duct outlet from windshield (Figure 4.1), 2) Opening: opening of outer duct outlet (Figure 4.2) and 3) Angle: angle between duct outlet and tangent to windshield (Figure 4.3).

Based on these, a certain number of geometries are generated and simulated. The upper and lower limits of the design parameters are presented in Table 4.1.

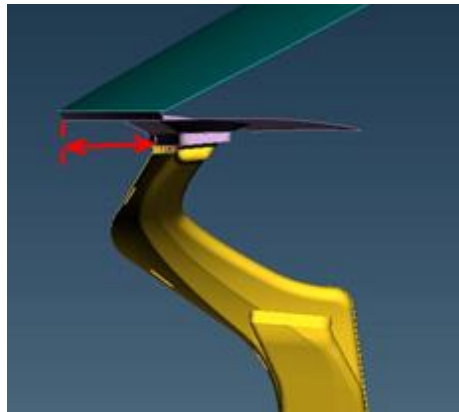


Figure 4.1: Design parameter: Distance

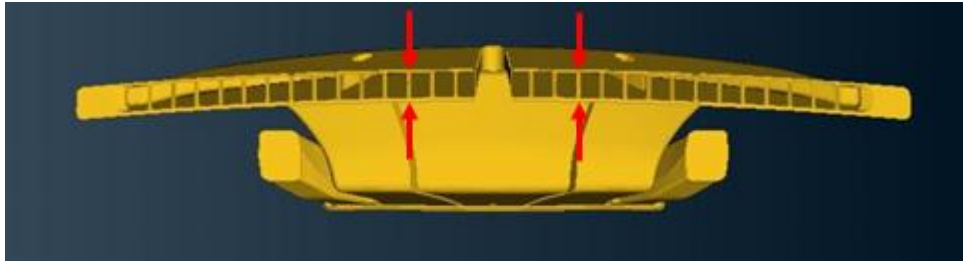


Figure 4.2: Design parameter: Opening

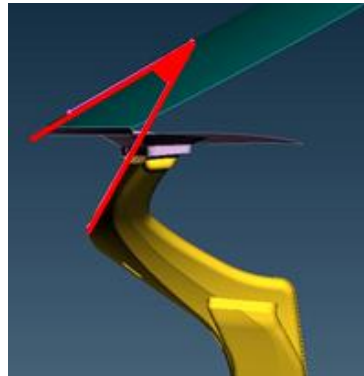


Figure 4.3: Design parameter: Angle

Table 4.1: Design parameters values

Parameter	Lower limit	Nominal value	Upper limit
Distance [mm]	-25%	-	240%
Opening [mm]	-26%	-	48%
Angle [deg]	-35%	-	30%

4.3 *Design Constraints*

After selecting the design parameters, appropriate constraints should be set in order to achieve a desired and realistic optimal geometry to manufacture. In the studied case, there are two kinds of constraints: a) geometric and b) flow related and specifically the total pressure drop.

4.3.1 *Geometric Constraints*

Geometric constrains (construction procedure, operability,, fitting in front component, aesthetic etc.) concern the shape of the duct and are determined by collaboration between designers and engineers. In the studied case, three geometric constraints are imposed, namely: 1) Frozen position and shape of inlet of defroster (Figure 4.4) in order to reduce costs of altering HVAC unit, 2) Parallel edges of outlet of defroster (Figure 4.5) for aesthetics reasons and 3) Constant distance and opening throughout the width (Figure 4.6) for IP constraints and aesthetic reasons. All the generated duct geometries must respect these constraints.

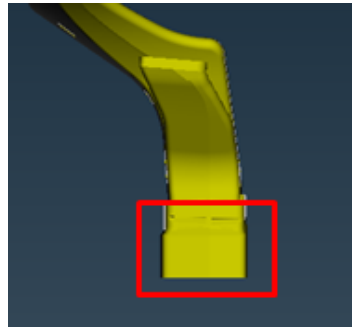


Figure 4.4: Constraint 1

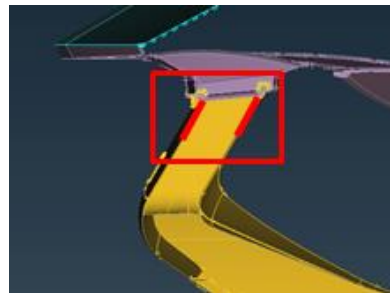


Figure 4.5: Constraint 2

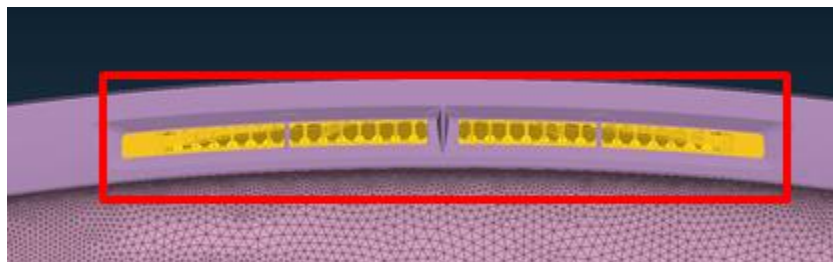


Figure 4.6: Constraint 3

4.3.2 Total pressure Drop

The fan of the defrosting system is driven by the car engine power or by electricity power in the case of an electric car. Thus, higher efficiency of this system means that it has the desired operation with the lowest possible power consumption. According to this, the new duct geometries should have equal or lower total pressure drop compared to the starting (reference) configuration. This is the flow related constraint used in this study.

4.4 Sampling of Design Space

Having set the design parameters and constraints, the determination of the geometries to be studied from the entire design space, is possible.

A three-level design is proposed so as to model possible curvature in the response function and to handle the case of nominal factors at 3 levels.

Having 3 design variables [k] allows to run a full factorial experiment of 3 levels (3^k factorial design) which results to $3^3=27$ new designs. The design parameters values for these designs are depicted in Table 4.2.

Table 4.2: Design parameters values of the 27 new designs

Distance	Opening	Angle	Distance	Opening	Angle	Distance	Opening	Angle
-25%	-26%	-35%	-25%	-26%	0%	-25%	-26%	30%
-25%	0%	-35%	-25%	0%	0%	-25%	0%	30%
-25%	48%	-35%	-25%	48%	0%	-25%	48%	30%
0%	-26%	-35%	0%	-26%	0%	0%	-26%	30%
0%	0%	-35%	0%	0%	0%	0%	0%	30%
0%	48%	-35%	0%	48%	0%	0%	48%	30%
240%	-26%	-35%	240%	-26%	0%	240%	-26%	30%
240%	0%	-35%	240%	0%	0%	240%	0%	30%
240%	48%	-35%	240%	48%	0%	240%	48%	30%

4.5 Preparation of New Geometries

Having determined the values of the design parameters for the 27 geometries, it is now possible to create these geometries in order to evaluate them and find the most promising ones.

New geometries can be generated by two methods: 1) generation with CAD and b) changing through morphing the original surface mesh. In this study, the morphing procedure is used and the new geometries meshes will result from the mesh of the original duct.

4.5.1 *CAD*

A CAD software is used in order to create the new geometry based on the design parameters values. The CAD data are used to create a water tight surface mesh which finally leads to surface and volume mesh and the evaluation can be performed (Figure 4.7).

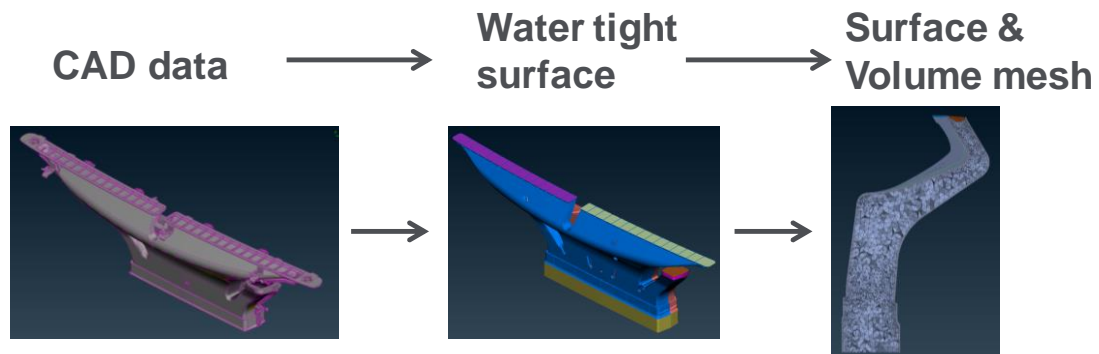


Figure 4.7: CAD based creation of new geometries

The major disadvantage of this method is that it is a very slow procedure and requires every time the construction of a different mesh each time a new geometry must be evaluated.

4.5.2 *Morphing*

Another approach is to use morphing tools in order to create the new geometries based on existing mesh of the original duct (Figure 4.8).

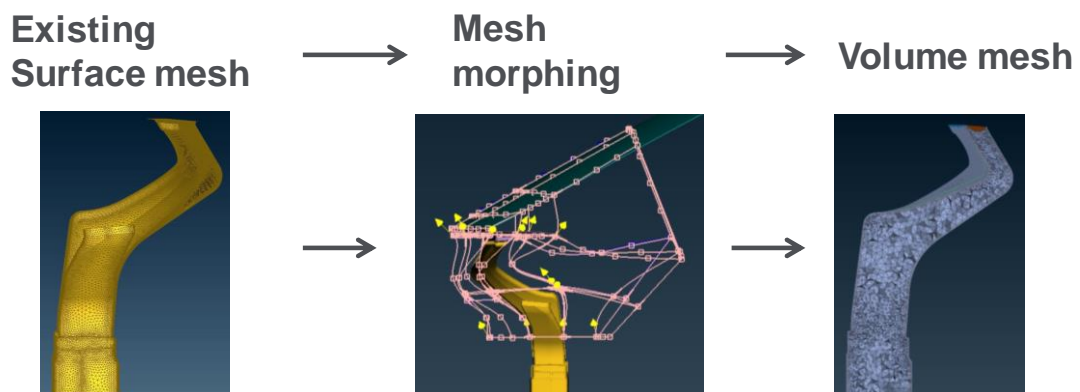


Figure 4.8: Creation of new geometries based on mesh morphing

The advantages of this method is that once morphing parameters are set, the morphing procedure is very quick and mesh quality improvement can take place without altering significantly the initial mesh.

The disadvantages of this procedure is that setting morphing parameters can be difficult based on some requirements. Another drawback is that morphing

can result to unrealistic mesh geometries which require manual check and evaluation (attention is needed when setting morphing parameters and generating mesh geometries) (Figure 4.9).

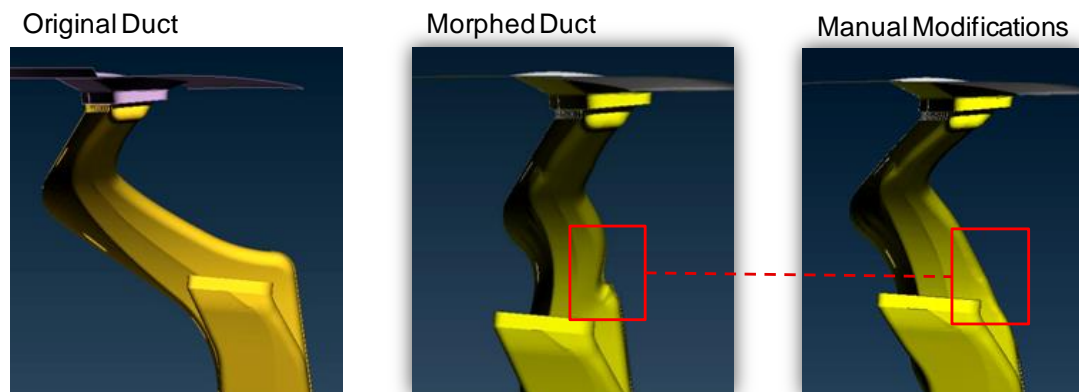


Figure 4.9: Manual morphing modifications

In order to reduce the generation of unrealistic geometries, a special entity in meshing, the nested elements must be used. They are entities that act as constraints during the morphing actions (Figure 4.10). A nested element acts as an un-deformable shape. The movement in the 3D space that the nested element are allowed to do, depend on the constraints that are imposed to them by means of degrees of freedom.

In this study, the nested elements ensure that the curvature of the windshield curve on axis y remains constant during morphing. The elements on the windshield are dependent of the single element in the lower part of the duct. Translation and rotation around all three axes is not allowed.

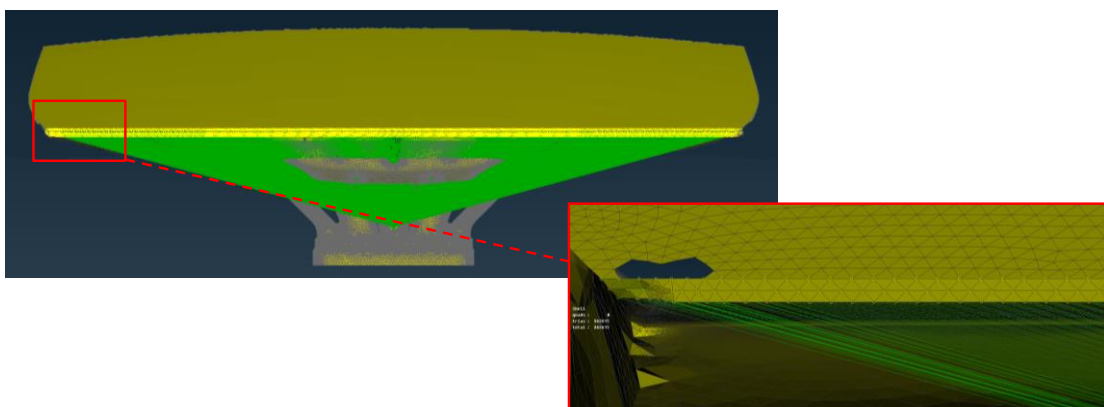


Figure 4.10: Nested Elements

Morphing tools provide two options: a) box morphing and b) direct fit morphing.

- *Box morphing*

Box morphing is performed via boxes that can be reshaped by moving control points that are located along their edge. Multiple hexahedral morphing boxes following the shape of the structure are created around the part of assembly that is intended to be morphed. Moving or sliding control points results in the morphing on the entities inside the morphing box along the desired direction (Figure 4.11). In this method, linked boxes can be used in models where symmetry appears, but morphing box parameters can result in conflicting displacements.

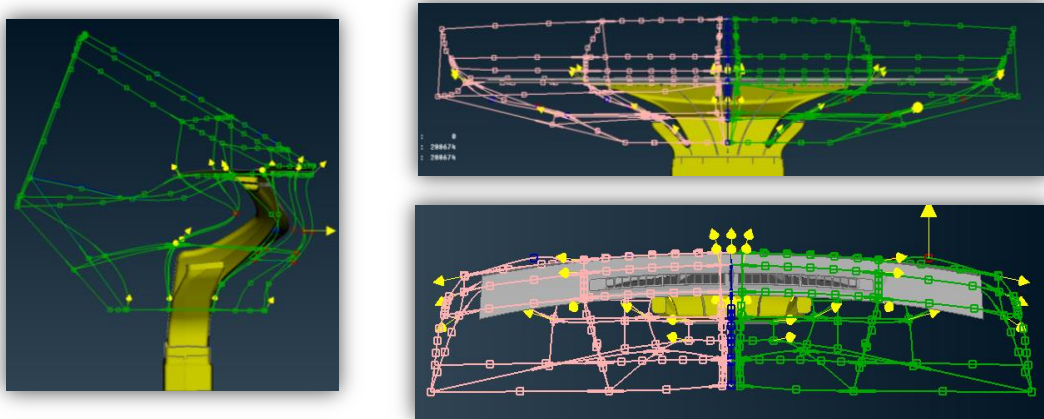
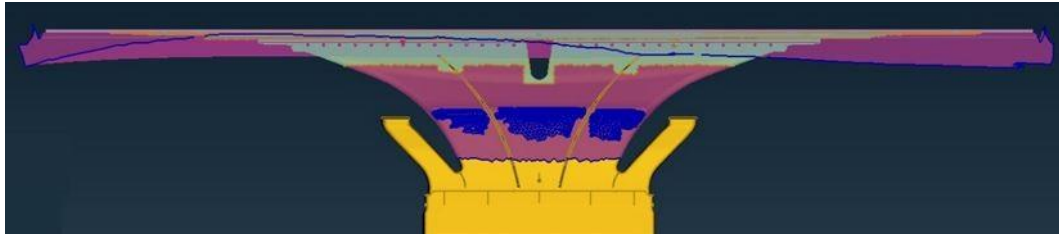


Figure 4.11: Box morphing

- *Direct fit morphing*

Direct fit morphing is performed without using boxes; it can be used for local modifications or complete assemblies, as it can guarantee smooth continuity (Figure 4.12). The specified part of the model can be displaced as a non-deformable body while the surrounding area absorbs the movement without damaging the continuity of the model.



Purple = Morphed entities **Light Blue = Control entities**
Blue = Bounds **Yellow = Frozen entities**

Figure 4.12: Direct fit morphing

Parametric morphing

By defining the desired morphing actions as parameters, the user can enforce desired shape modifications by simply changing the numerical input values of the appropriate parameters. This functionality is highly useful in DoE studies.

Morphing parameters

For performing the mesh morphing, the definition of the morphing parameters is necessary. For the studied case, morphing parameters derive from geometry constraints and are:

- Distance (used for Direct Fit Morphing)
- Opening (used for Direct Fit Morphing)
- Angle (used for Box Morphing)

4.6 Solver & Mesh

For the solution of the flow, the construction of mesh is mandatory. To speed up building the model, CAD data is only used for parts where high accuracy is needed. Laser scanned surface data is used for the rest of interior (Figure 4.13).

After geometry clean-up, CAD data is precisely stitched to STL data in ANSA software running in TME. Mesh refinement boxes are defined to achieve high accuracy where needed while balancing overall computational cost (Figure 4.14).

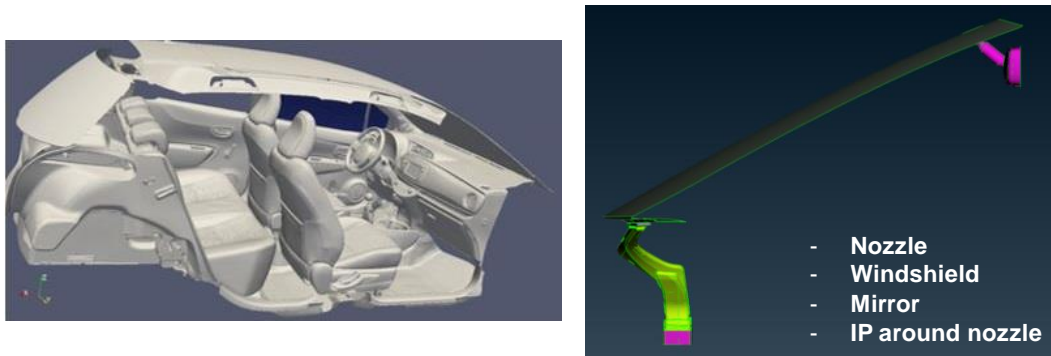


Figure 4.13: CAD data for mesh construction

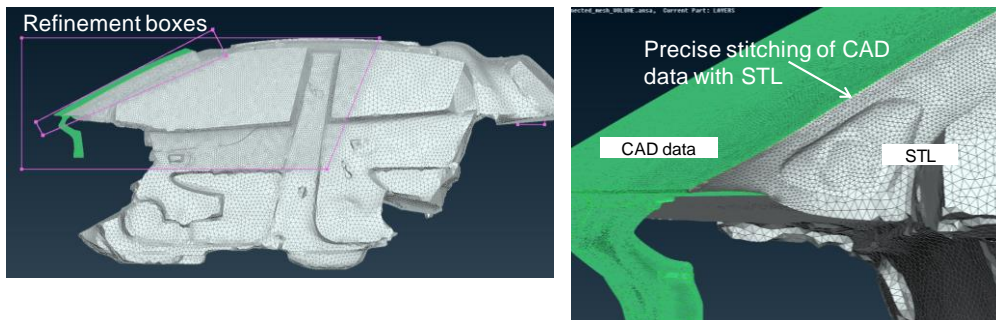


Figure 4.14: CAD data to STL in ANSA

The volume mesh is a combination of structured layers and unstructured mesh. Layers are generated to simulate with accuracy the flow in the boundary layer (Figure 4.18).

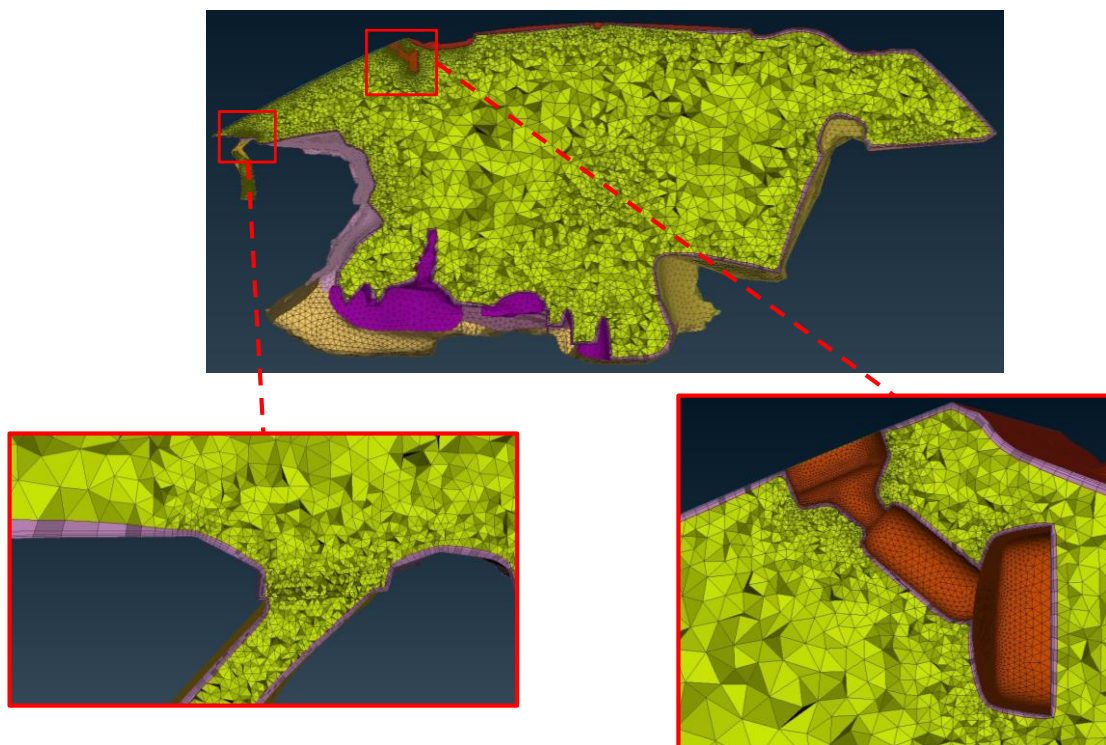


Figure 4.15: Volume mesh

After the generation of the mesh for each desired geometry, the solution of the flow can be obtained by solving the Navier-Stokes equations. The general solving procedure is depicted in Figure 4.16. Any other useful data, can be computed via post-processing. The used software is openFOAM and the solver is the simpleFoam.

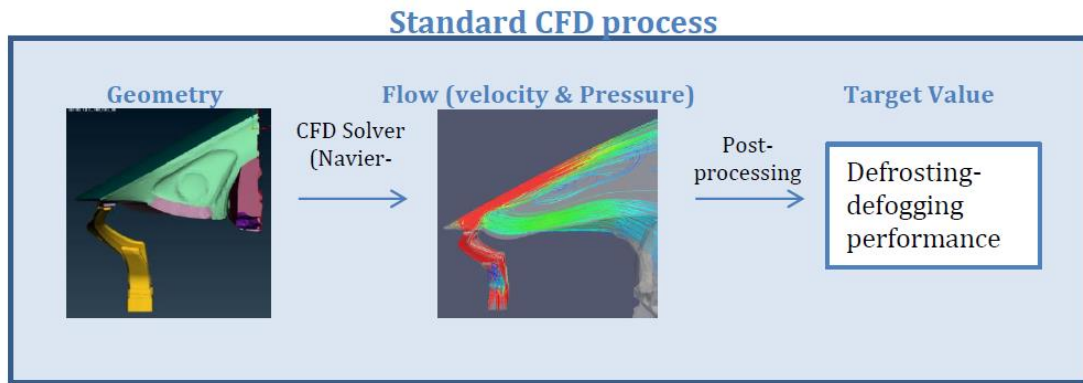


Figure 4.16: The general solving procedure

Before the solving, with the pre-processing procedure, boundary flow conditions concerning the inlet and the outlet flow are set. The flow velocity is fixed with a zero gradient for pressure at the inlet and, at the outlet, the gauge pressure is 0 atm with a zero gradient for velocity (Figure 4.17).

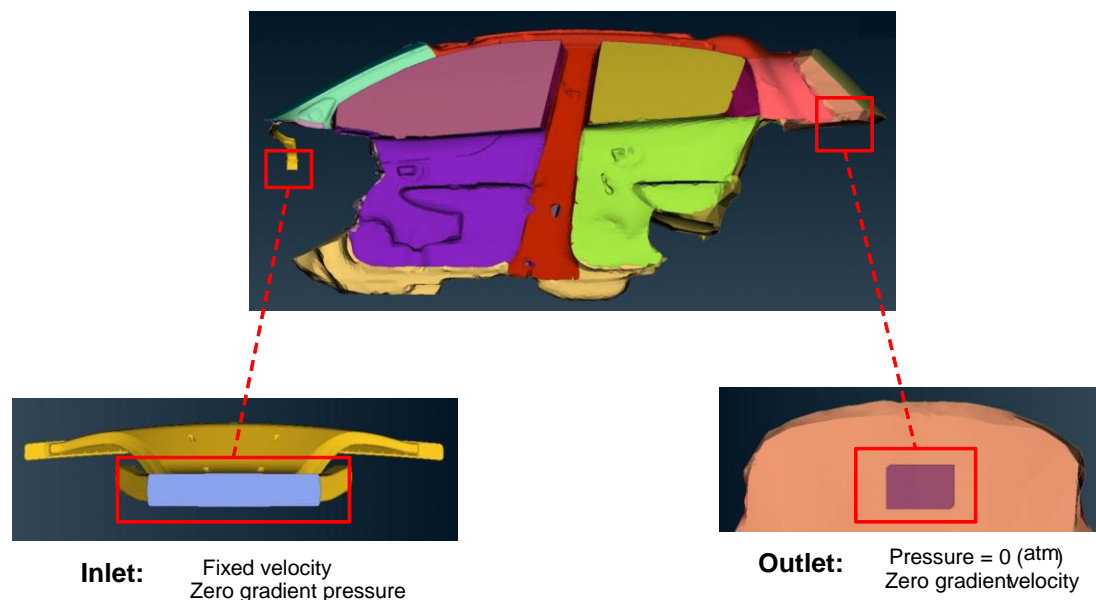


Figure 4.17: Pre-processing procedure

After the pre-processing procedure, the solution of the flow is achieved by solving the Reynolds-Averaged Navier–Stokes (RANS) equations assuming steady state. Flow is assumed incompressible and the $k-\epsilon$ turbulence model is used. Finally, 2nd order accuracy is chosen.

The solving phase is successful if all values are converging to a stable result and that the residuals of the Navier-Stokes equations are very small (below $1E-4$ and $1E-6$ for pressure and velocity respectively).

In addition to the residuals, the velocity and pressure at a probed location as well as the value of the objective function are monitored.

After solving the flow, the computation of other useful parameters (like velocity pattern) is able through a post-processing procedure as it can be seen in Figure 4.18. For example, by generating streamlines, it can be concluded that recirculation occurs in the lower half of the windshield while at the upper half the velocity magnitude is almost zero (Figure 4.18).

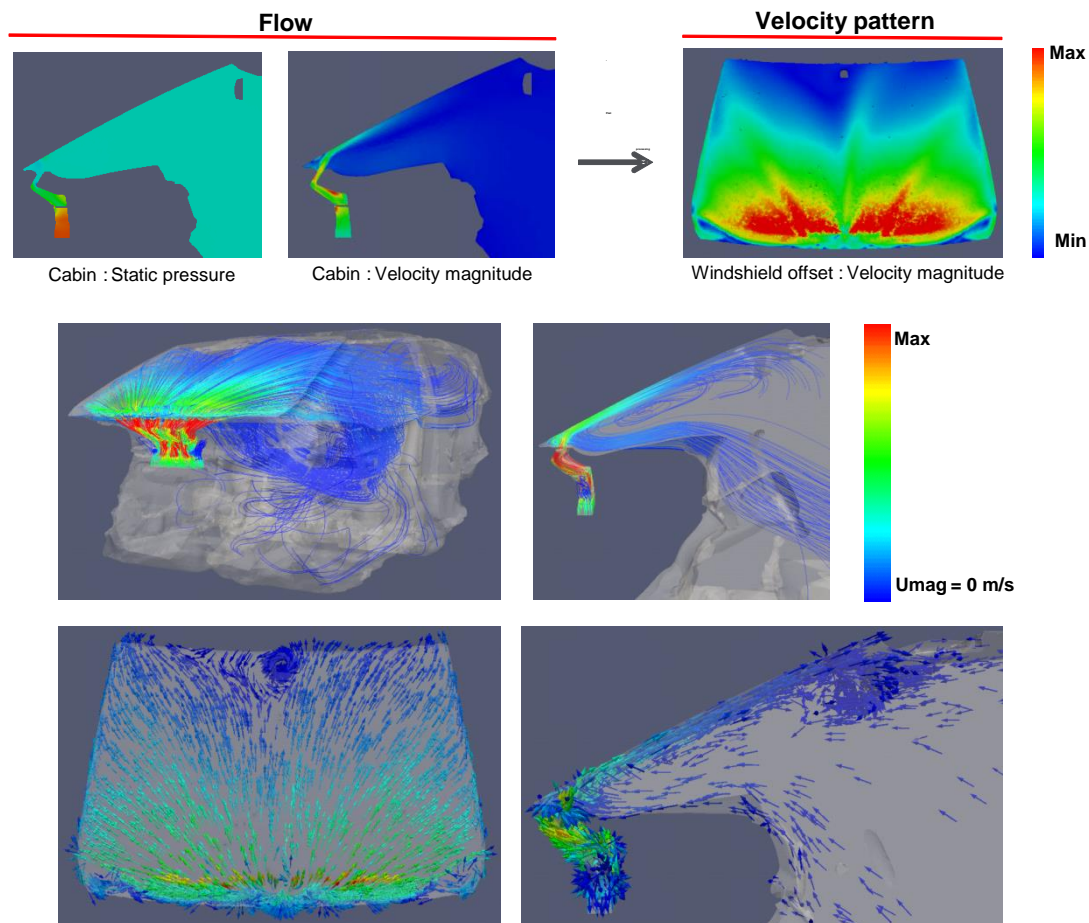


Figure 4.18: Post-processing results

4.7 Target & Objective Function

The target of this study is to improve the velocity pattern of the air close to the windshield (Figure 4.20). In other words, the aim is to achieve more uniform distribution of the velocity and increase its magnitude on the weakest areas (Figure 4.19), which for the current design is mostly the upper part of the windshield (Figure 4.21). At the same time, as stated previously, the new duct geometries should have equal or lower total pressure drop compared to the starting (reference) configuration.



Figure 4.19: Target of study

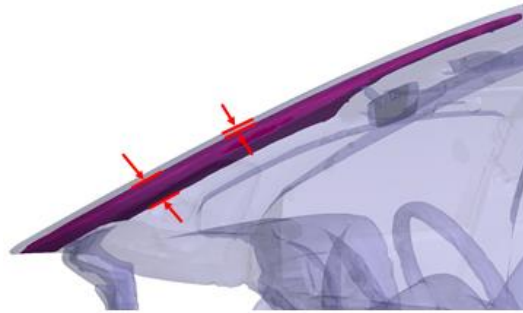


Figure 4.20: Area of interest

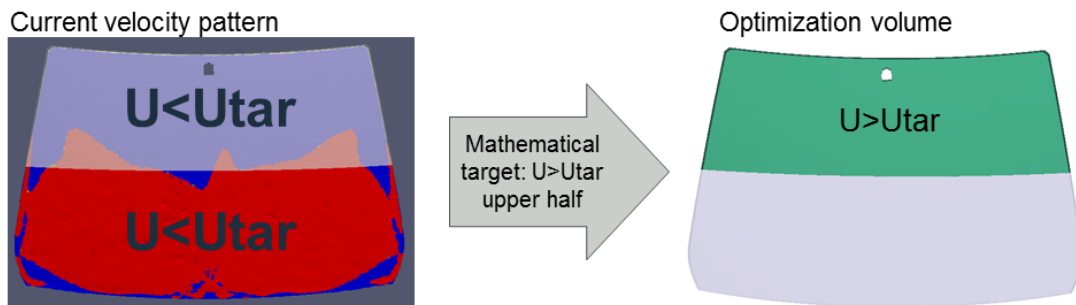


Figure 4.21: Optimization target: improvement of velocity magnitude in the upper half windshield

The evaluation of each new shape is performed by the use of objective/cost functions. In a minimization problem like the studied one, lower value of the objective function means better performance.

The used objective functions are described below.

$$F_{obj} = \frac{1}{2} \int_{\Omega_{tar}} (u_i^2 - u_{i,tar}^2)^2 d\Omega_{tar} \quad 4.1$$

Or, in a general form,

$$F_{obj} = \int_{\Omega_{tar}} F_{obj,\Omega_{tar}} d\Omega_{tar} \quad 4.2$$

The volume-averaged total pressure losses (F_{P_t}) and the fluid power dissipation (F_{P_L}) can be computed by:

$$F_{P_t} = \int_{S_i} \left(p + \frac{1}{2} u_k^2 \right) u_i n_i dS - \int_{S_o} \left(p + \frac{1}{2} u_k^2 \right) u_i n_i dS$$

\uparrow
 n_i is directed outwards

$$F_{P_L} = \int_{\Omega} \left[\frac{\nu + \nu_t}{2} \left(\frac{\partial u_i}{\partial x_j} + \frac{\partial u_j}{\partial x_i} \right)^2 \right] d\Omega$$

4.3

Proving that the volume-average total pressure losses are the equivalent of the fluid power dissipation will allow us to use the existing dissipated power objective function and therefore, reduce the need to interfere further with the source code.

The analysis applies to shape optimization and the total kinetic energy along as its time derivative is:

$$E_{kin} = \int_{\Omega} \frac{1}{2} u_i^2 d\Omega$$

$$\frac{\partial E_{kin}}{\partial t} = \int_{\Omega} u_i \frac{\partial u_i}{\partial t} d\Omega$$

At the same time, the momentum equation:

$$R_i^u = \frac{\partial u_i}{\partial t} + u_j \frac{\partial u_i}{\partial x_j} + \frac{\partial p}{\partial x_i} - \frac{\partial \tau_{ij}}{\partial x_j} = 0$$

$$u_i \frac{\partial u_i}{\partial t} = \underbrace{u_i u_j \frac{\partial u_i}{\partial x_j}}_{\text{term(1)}} + \underbrace{u_i \frac{\partial p}{\partial x_i}}_{\text{term(2)}} - \underbrace{u_i \frac{\partial}{\partial x_j} \left[(\nu + \nu_t) \left(\frac{\partial u_i}{\partial x_j} + \frac{\partial u_j}{\partial x_i} \right) \right]}_{\text{term(3)}}$$

4.4

$$\text{term(1)} = \frac{1}{2} u_j \frac{\partial (u_i)^2}{\partial x_j} = \frac{1}{2} \frac{\partial u_i^2 u_j}{\partial x_j}$$

$$\text{term(2)} = \frac{\partial (u_i p)}{\partial x_i}$$

$$\text{term(3)} = u_i \frac{\partial}{\partial x_j} [(\nu + \nu_t) S_{ij}] = \frac{\partial}{\partial x_j} [(\nu + \nu_t) u_i S_{ij}] - (\nu + \nu_t) S_{ij} \frac{\partial u_i}{\partial x_j}$$

where $\frac{\partial u_i}{\partial x_j} \neq 0$

should be satisfied and so does the continuity equation:

$$-\frac{\partial u_i}{\partial x_i} = 0$$

Therefore

$$\begin{aligned} u_i \frac{\partial u_i}{\partial t} &= \frac{1}{2} \frac{\partial u_i^2 u_j}{\partial x_j} + \frac{\partial(u_i p)}{\partial x_i} - \frac{\partial}{\partial x_j} [(v + v_t) u_i S_{ij}] + (v + v_t) S_{ij} \frac{\partial u_i}{\partial x_j} \\ &= \frac{\partial}{\partial x_j} \left[u_j \left(\frac{1}{2} u_i^2 + p \right) \right] - \frac{\partial}{\partial x_j} [(v + v_t) u_i S_{ij}] \\ &\quad + (v + v_t) S_{ij} \frac{\partial u_i}{\partial x_j} \end{aligned} \quad 4.5$$

The Frobenius inner product of S_{ij} & $\frac{\partial u_i}{\partial x_j}$ is:

$$\begin{aligned} \frac{\partial u_i}{\partial x_j} S_{ij} &= \frac{\partial u_i}{\partial x_j} \left(\frac{\partial u_i}{\partial x_j} + \frac{\partial u_j}{\partial x_i} \right) = \frac{\partial u_i}{\partial x_j} \frac{\partial u_i}{\partial x_j} + \frac{\partial u_i}{\partial x_j} \frac{\partial u_j}{\partial x_i} \\ &= \frac{1}{2} \frac{\partial u_i}{\partial x_j} \frac{\partial u_i}{\partial x_j} + \frac{1}{2} \frac{\partial u_j}{\partial x_i} \frac{\partial u_j}{\partial x_i} + \frac{\partial u_i}{\partial x_j} \frac{\partial u_j}{\partial x_i} \\ &= \frac{1}{2} \left(\frac{\partial u_i}{\partial x_j} \right)^2 + \frac{1}{2} \left(\frac{\partial u_j}{\partial x_i} \right)^2 + \frac{\partial u_i}{\partial x_j} \frac{\partial u_j}{\partial x_i} = \frac{1}{2} \left(\frac{\partial u_i}{\partial x_j} + \frac{\partial u_j}{\partial x_i} \right)^2 \\ &= \frac{1}{2} S_{ij}^2 \end{aligned} \quad 4.6$$

Therefore it is proven that:

$$-\int_{S_{I,O}} \left(p + \frac{1}{2} u_i^2 \right) u_j n_j dS \cong \int_{\Omega} \frac{(v + v_t)}{2} S_{ij}^2 d\Omega \quad 4.7$$

$F_{Pt} \cong F_{PL}$

and the dissipated power is:

$$J = \int_{\Omega} \frac{(v + v_t)}{2} S_{ij}^2 d\Omega \quad 4.8$$

4.8 Results of DoE Study

After having constructed the evaluation tool for the new geometries, it is now possible to estimate the performance of the 27 ducts as they described in Table 4.2. The performance of original duct is depicted in Figure 4.22, while indicatively 3 out of 27 ducts along with their performance are depicted in Figure 4.23.

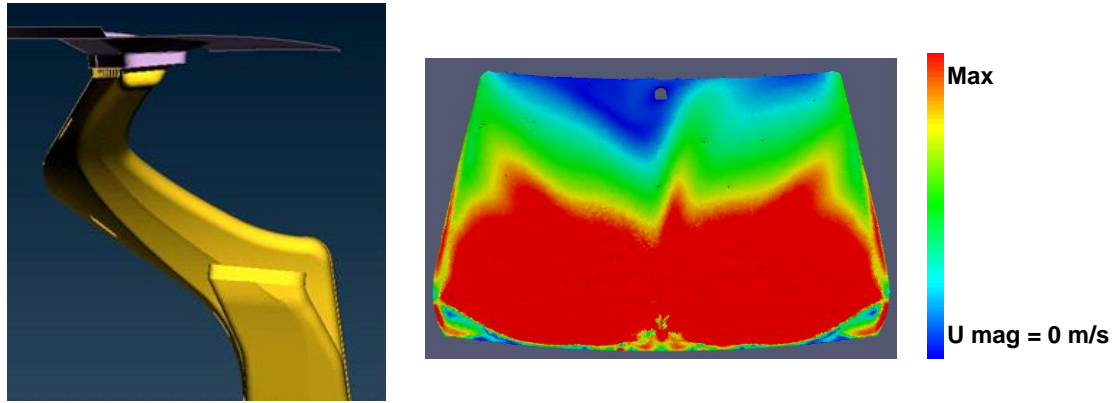


Figure 4.22: Air velocities for original duct

D: Distance O: Opening A: Angle	Duct appearance	Duct performance
D=-25% O=-26% A=-35%		
D=0% O=48% A=0%		
D=240% O=0% A=30%		

Figure 4.23: Geometry and performance of various ducts

From the examination of the performance of these 27 ducts, it can be concluded that:

- a) for constant angle and opening, distance increase is beneficial,
- b) for constant distance and opening, angle decrease is somehow beneficial,
- c) for constant angle and distance, opening values lower or equal to the original one give better performance.

In order to better assess the performance of these 27 ducts, the objective function and the total pressure drop are computed for each duct. The percentage difference from original for the objective function and the total pressure drop is depicted in Figure 4.24 through Figure 4.26.

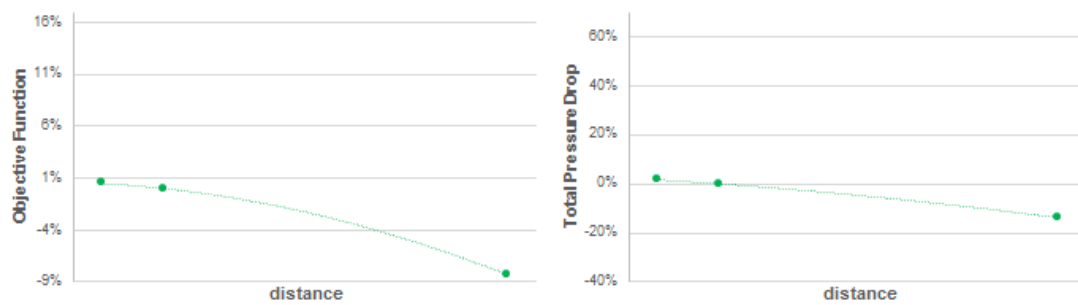


Figure 4.24: Objective function and total pressure drop difference from original duct for original opening and angle values and variable distance value

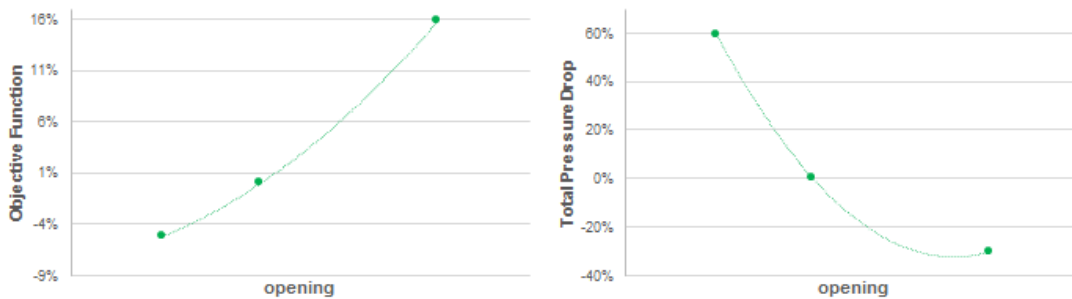


Figure 4.25: Objective function and total pressure drop difference from original duct for original distance and angle values and variable opening value

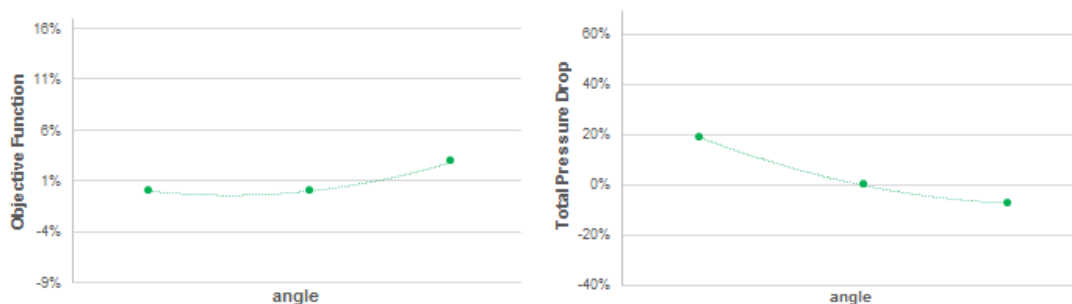


Figure 4.26: Objective function and total pressure drop difference from original duct for original distance and opening values and variable angle value

It is concluded that Distance and Opening have a significant effect on objective function and total pressure drop: higher distance value results to lower objective function and total pressure drop values (Figure 4.24), higher opening value results to higher objective function and lower total pressure drop values (Figure 4.25). Finally, Angle has little effect on objective function and total pressure drop (Figure 4.26).

The performance of the 27 geometries for the objective function and the total pressure drop is summarized in Figure 4.27.

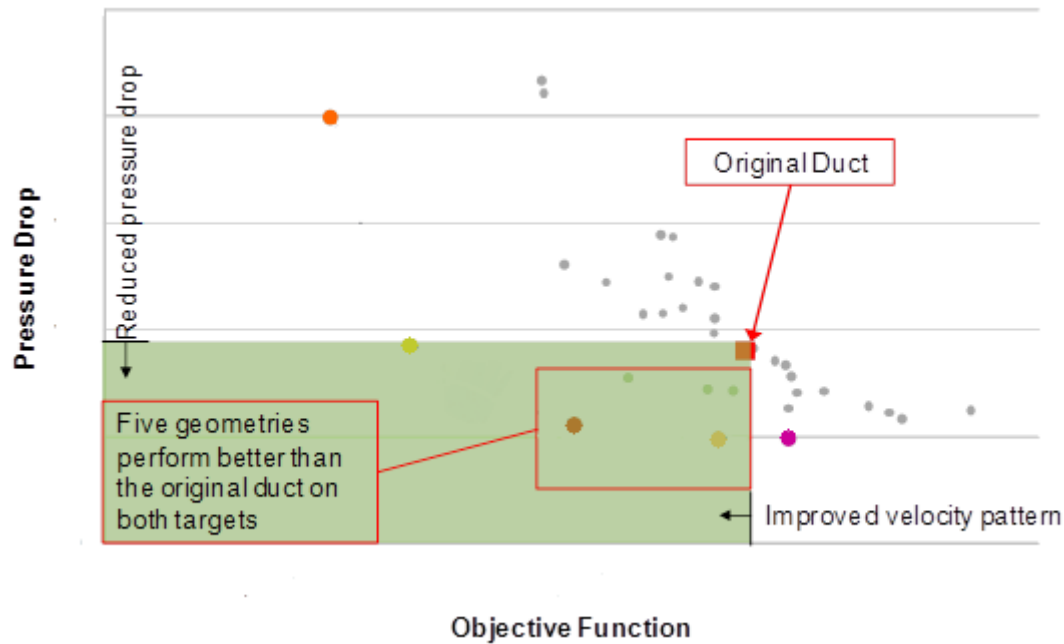


Figure 4.27: Performance of the 27 geometries

In order to evaluate the combined effect on performance from the simultaneous variation of parameters values, an appropriate parametric study was carried out in which one parameter takes a constant value while the values of the other two are varied (Figure 4.28).

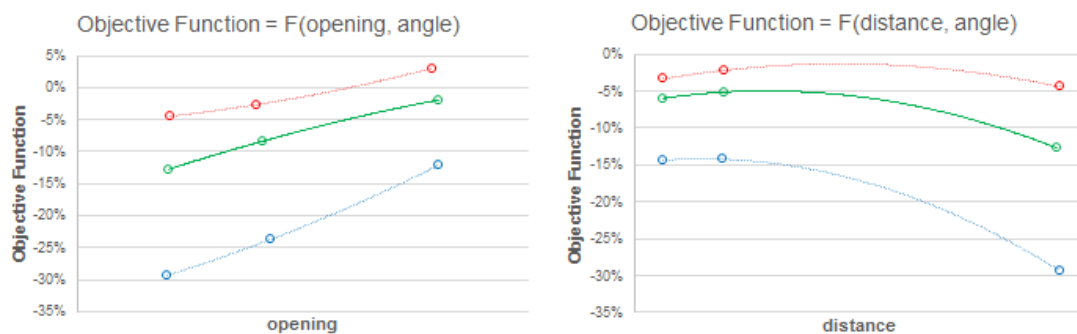


Figure 4.28: Results of parametric study

From this study it is concluded that:

- a) Assigning the minimum value to the opening parameter results always to better velocity patterns but higher total pressure drop as well.
- b) As the value of angle increases, the distance and opening parameters have less effect on the objective function.
- c) Although the parameters are independent, their contribution to the objective function is not.
- d) The objective function approximation must contain interaction terms to serve as a suitable approximation to the true relationship.

In order to find the optimal duct geometry, an optimization procedure is needed by which the performance of each new duct is quantified and the geometry is alternated accordingly.

The computation of the duct performance by solving the RANS equations is costly, especially having in mind that many calculations should be performed due to the evaluation of every new geometry which makes this procedure time expensive.

To overcome this problem, the regression model which can approximate the precise performance value will be used as an evaluation tool. In this case, the computation of the objective function is performed only for the most promising solutions. An indication of the computation cost difference between the two methods is depicted in Figure 4.29. The mathematical expression of this tool is:

$$y = \sum_{i=1}^3 a_{3i}x_i + \sum_{i=1}^3 a_{3i-1}x_i^2 + \sum_{i=3}^3 a_{3i-2}x_i^3 + \sum_{i=1}^3 \sum_{\substack{j=2 \\ i < j}}^3 a_{i+(j-2)+9}x_i x_j \quad 4.9$$

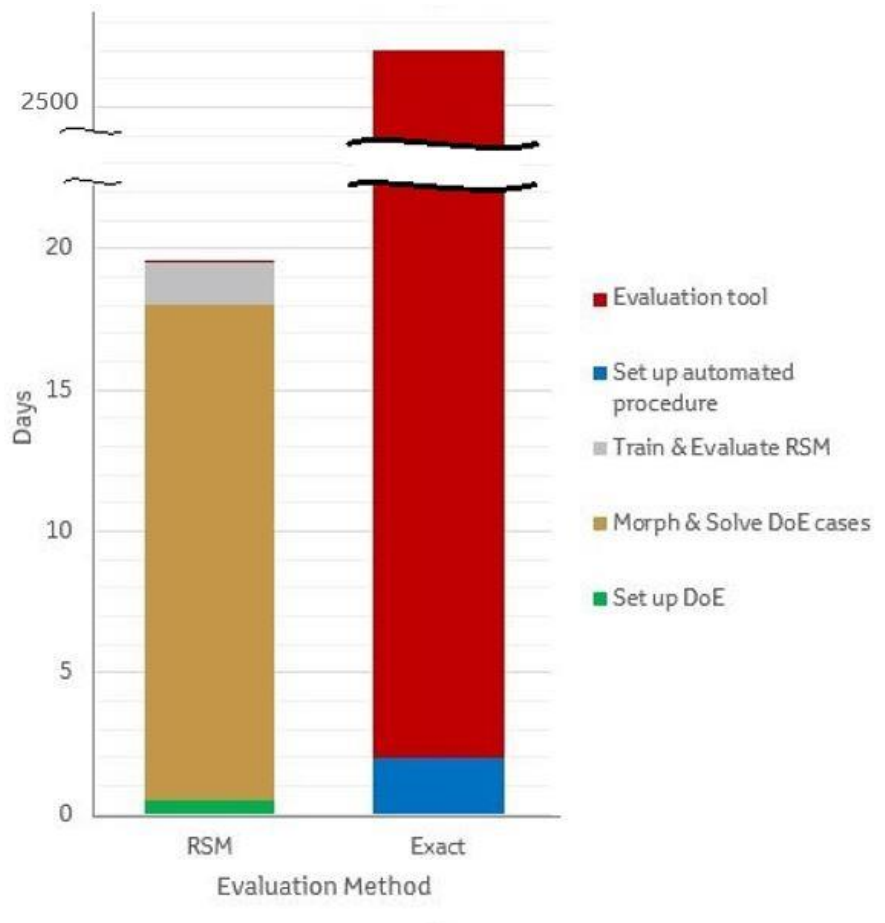


Figure 4.29: Comparison between the exact and the RSM evaluation methods

The determination of the coefficients (training) of this tool is performed by the use of a software developed by the PCOpt/NTUA which is fed with the value of the objective function for the corresponding geometries. The training procedure is depicted in Figure 4.30.

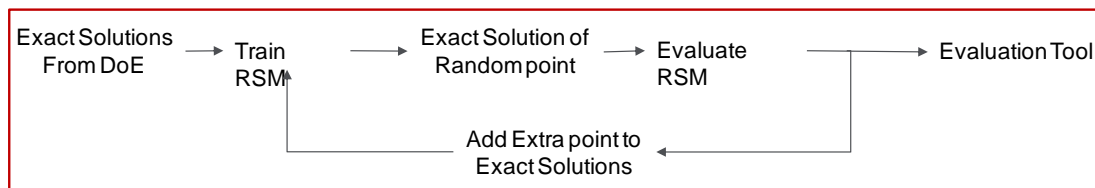


Figure 4.30: Training procedure of the evaluation tool

The optimal geometry that is derived from the RSM tool can then be fed into an optimization procedure that relies on the numerical solution of the RANS equations. In this way, a good approximation of the best geometry can be found by RSM, which then can be further optimized by a more precise tool.

To ensure RSM is accurate, 8 more duct geometries are taken into account which correspond to the 8 vertices of the inner cube concerning the studied design space (Table 4.3).

Table 4.3: Design parameters values of the 8 new designs

Distance	Opening	Angle	Distance	Opening	Angle
-14%	-14%	-19%	72%	-14%	-19%
-14%	-14%	13%	72%	-14%	13%
-14%	22%	-19%	72%	22%	-19%
-14%	22%	13%	72%	22%	13%

4.9 EASY Loop

In order to be able to optimize the duct geometry, an automated procedure which will alter the parameter values and evaluate the objective function, is mandatory. This procedure should evaluate the new geometries for two objectives, the objective function and the total pressure drop (a two-objective optimization).

In this study, EASY v2.0 is used which is a generic optimisation software developed by PCOpt, NTUA. Its chosen parameters values are:

- 20000 total calls of evaluation tool
- 10 bit per design variable – binary-Gray coding
- Parent and Offspring population size: 30/90
- Elite archive size: 15
- Tournament size and probability: 2/90%
- Crossover probability and mode: 95% - two points per variable
- Mutation probability: 2%

It should be mentioned that in this case, an off-line metamodel is used instead of solving RANS equation and its training procedure is depicted in Figure 4.31.

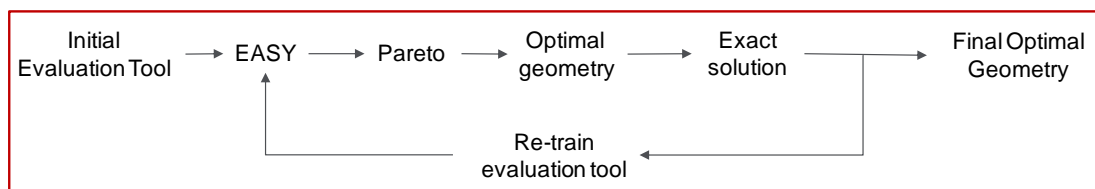


Figure 4.31: Training procedure of the evaluation tool with EASY

4.10 Results of the Optimization Loop

As it was described, the studied case is a multi-objective optimization problem and thus the best solutions will be appear on a Pareto Front. Points/solutions on Pareto Front dominate all other solutions. The optimal one will be searched on this front and will be chosen by the engineer taking into account other criteria.

For the studied case, the optimized solutions and their Pareto Front are depicted in Figure 4.32. As it can be seen, there are many geometries that perform better than the original duct.

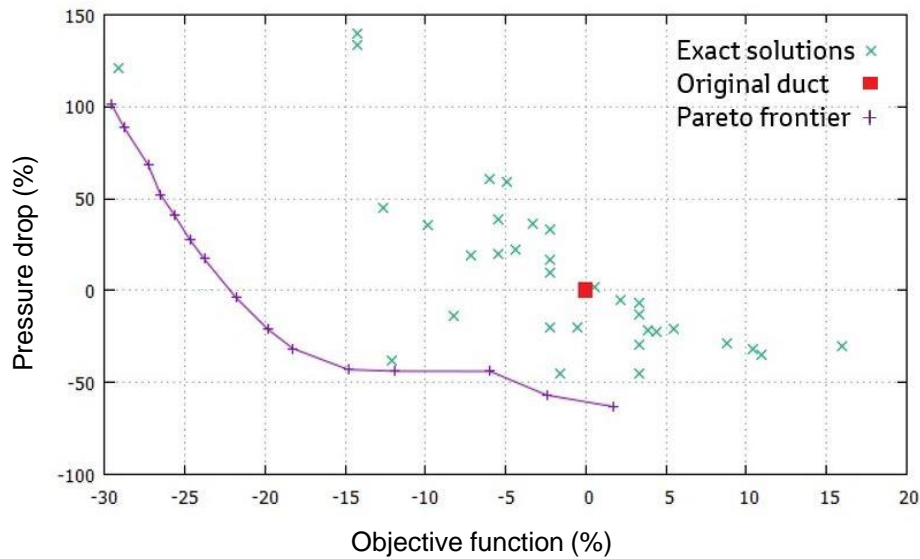


Figure 4.32: Optimized solution and Pareto Front

From the Pareto Front it can be seen that the lower the objective function value, the higher the total pressure drop is. In order to weight the two objectives and choose the optimal geometry, the following way of thinking is used: In order not to alter the load of the motor of the HVAC unit, total pressure drop value is desired to be the same as the original duct, and thus the optimal solution should have a zero percentile total pressure drop. In that way the optimal geometry is chosen (Figure 4.33) which has the same total pressure drop and a reduced objective function value by 22% compared to the original one.

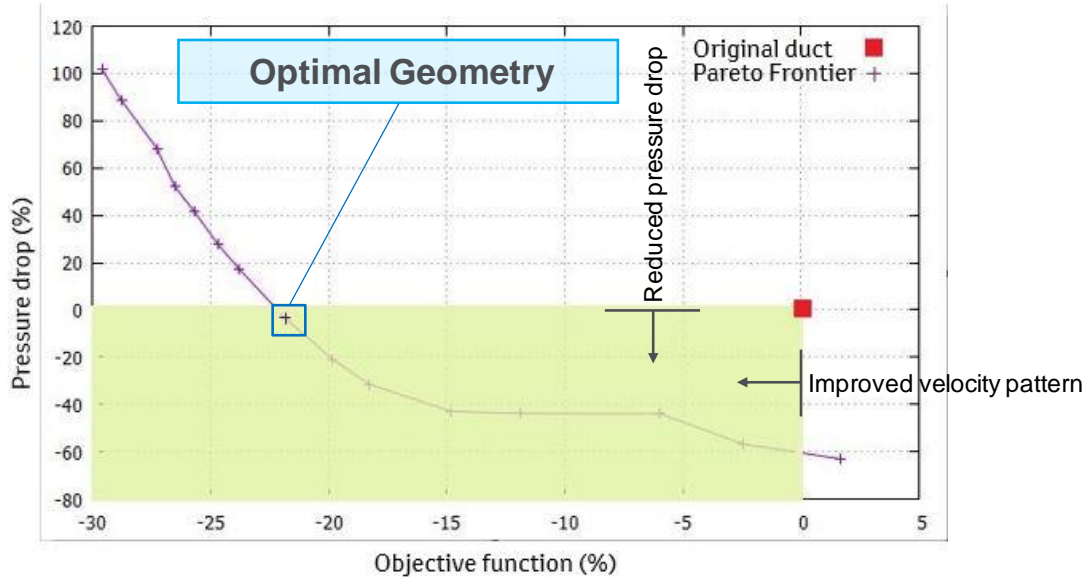


Figure 4.33: Optimal solution

4.11 Study of Optimized Duct Performance

The optimal solution has about the same total pressure drop compared to the original duct and lower objective function which means desired air velocity pattern through the windscreen. The optimal duct has lower Distance and Angle values and slightly higher opening value. The comparison between the two ducts, as well as the performance of the new one, is depicted in Figure 4.34 through Figure 4.36.

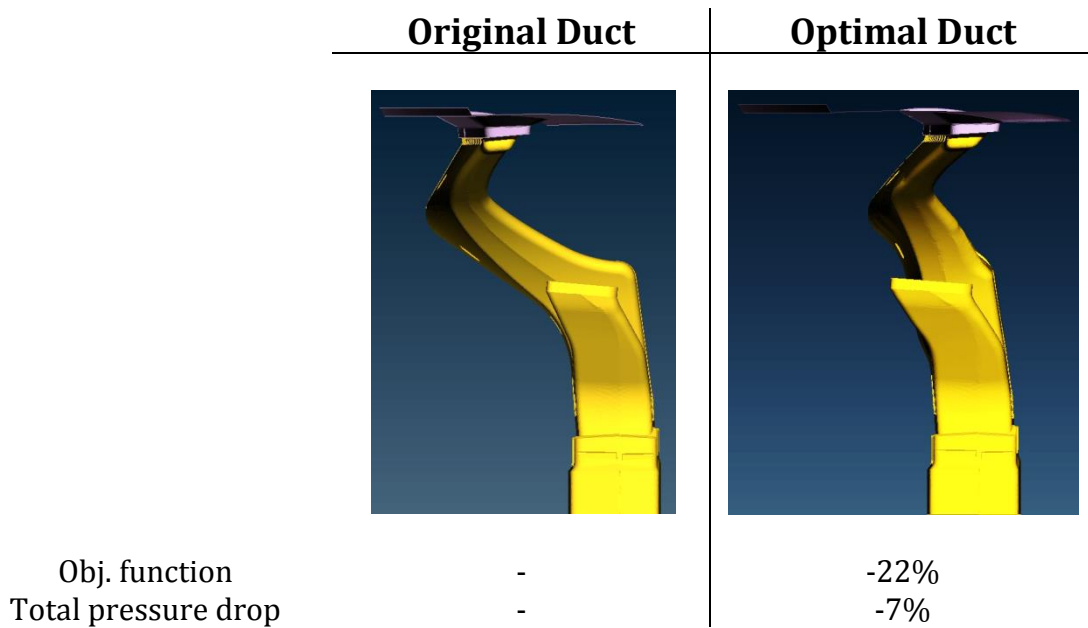


Figure 4.34: Optimal and original ducts

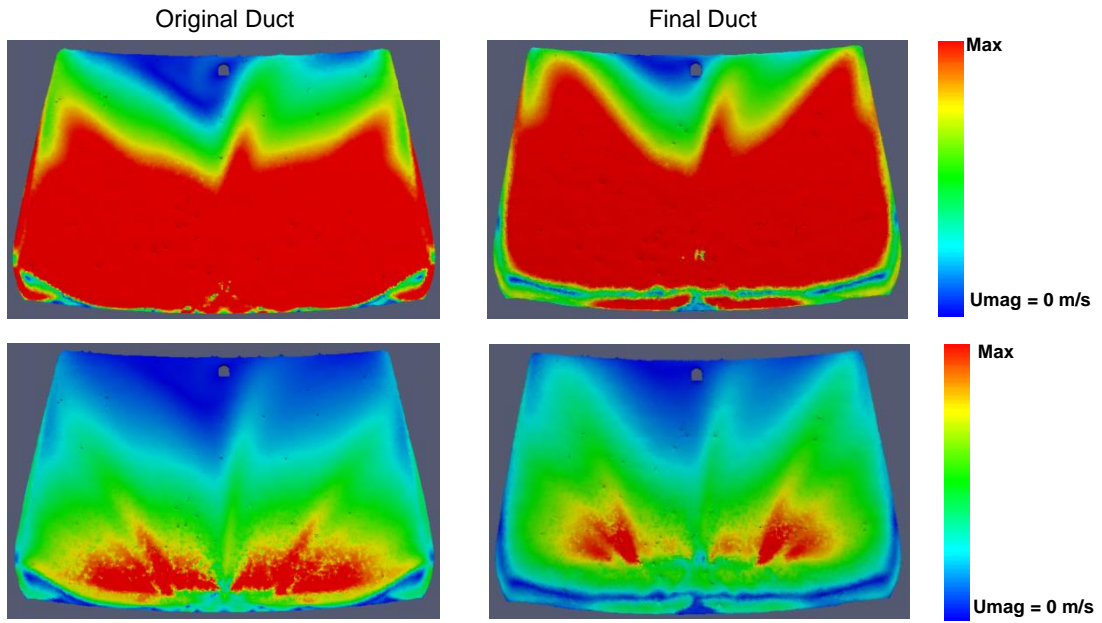


Figure 4.35: Velocity pattern of optimal duct

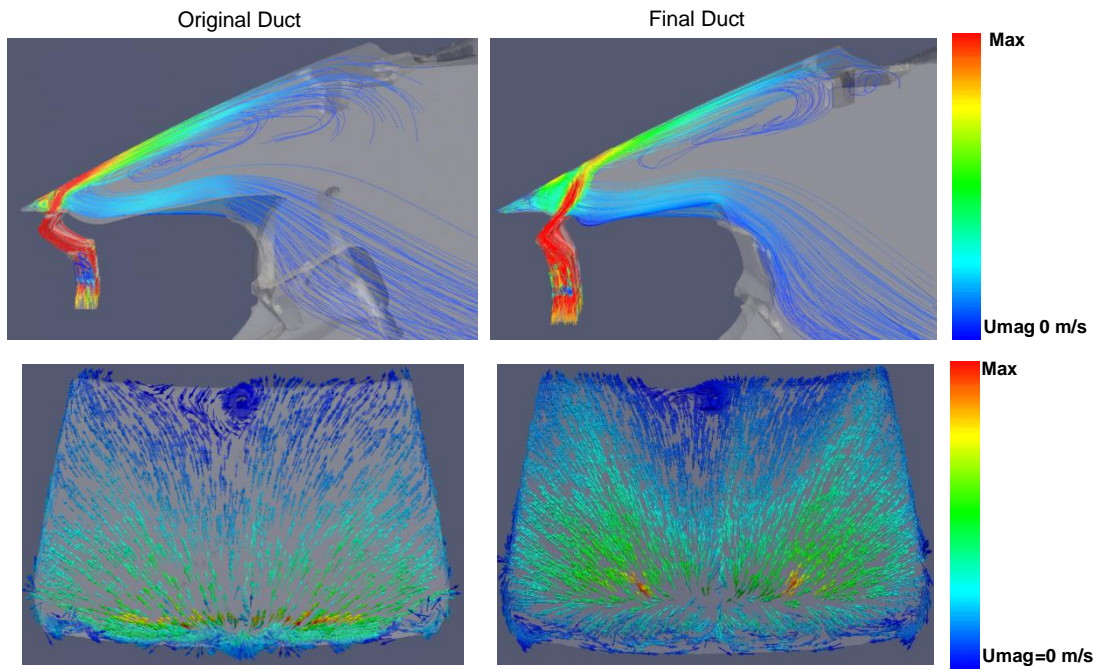


Figure 4.36: Streamlines & Velocity Glyph of optimal duct

5 Study of Width Parameter

5.1 Explanation of Width Parameter

Until now, the width of the duct (or its length alongside the windshield), was considered constant. As described in Chapter 1, new installations in the car (as a HUD display) require duct length reduction in order to fit properly. But, such a change will result in a different performance of the HVAC system and as a result the defrosting/defogging rate may not meet the requirements.

In order to add an HUD device in the studied car, the width of the duct should be altered. The appropriate duct width depends on the HUD geometry. In our case, the HUD geometry is not known and so, nothing but a preliminary study can be carried out to explore the effect of width on performance.

In this chapter, a study is carried out in order to find the effect of the width on the performance. Initially, a parametric study is performed altering the width in order to determine its effect on performance. For the most promising width case, a DoE study is carried out as it was done for the constant width case (Chapter 4). The next step, (the optimization with EASY) is not performed in this case, since the HUD geometry is not known and a more detailed optimization would be unnecessary and therefore a “waste” of computational power.



Figure 5.1: Examples of On-board (left) and In-Car (right) Head-Up Displays

5.1.1 Parameters

For the preliminary study, the values of design parameters are those of the initial duct. The width takes five values below the nominal one.

5.1.2 *Morphing*

For performing the mesh morphing, the determination of the morphing parameters is necessary. Along the three morphing parameters described in the previous chapter (Distance, Opening, Angle), one is added concerning the width of the duct. It is a Box Morphing parameter (Width, Figure 5.2).

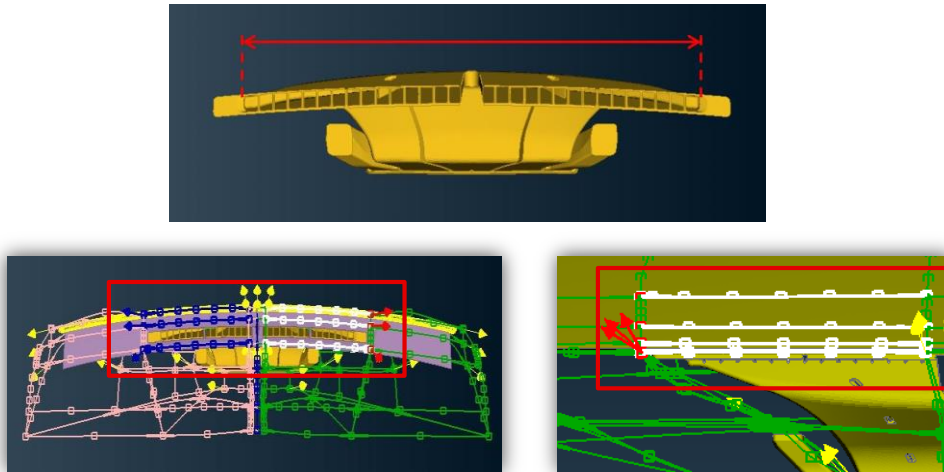


Figure 5.2: Box morphing parameter: Width

5.1.3 *Results*

The parametric study for the width gave the performance of 5 new duct geometries with reduced width. Their performance can be seen in Figure 5.3 and the total pressure drop in Figure 5.4.

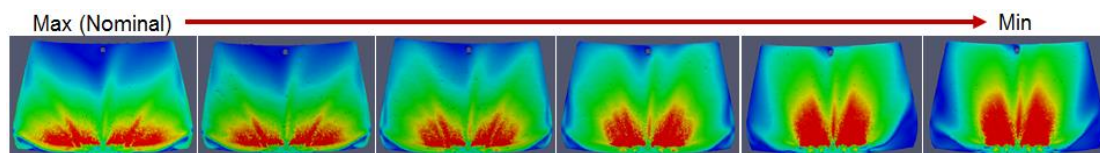


Figure 5.3: Velocity pattern of reduced width ducts

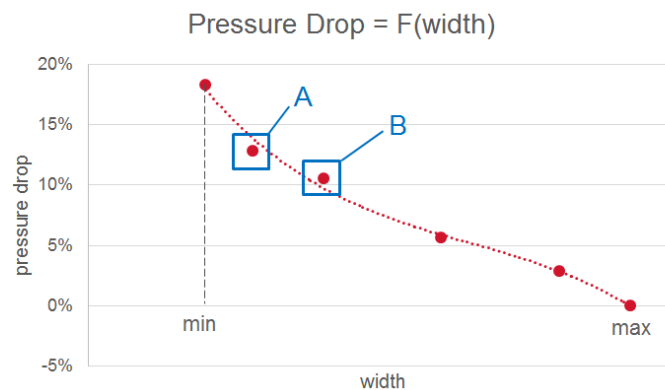


Figure 5.4: Total pressure drop of reduced width ducts

The ducts with width A and B have a sufficient width decrease compared with the original one and acceptable velocity patterns. The difference on velocity pattern between the original duct and duct A can be seen in Figure 5.5.

Figure 5.6 depicts streamlines of these two ducts. The difference on velocity pattern between the original duct and duct B can be seen in Figure 5.7.

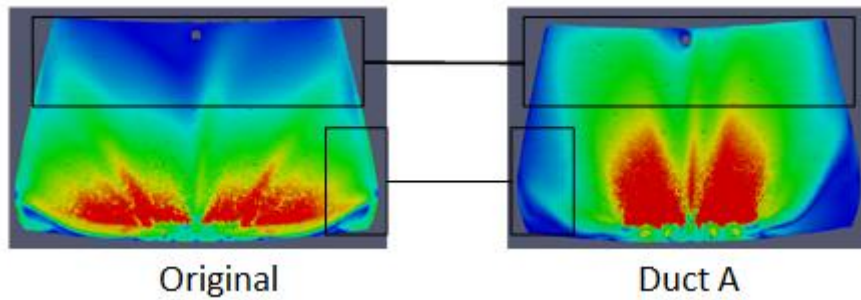


Figure 5.5: Velocity patterns of original duct and duct A

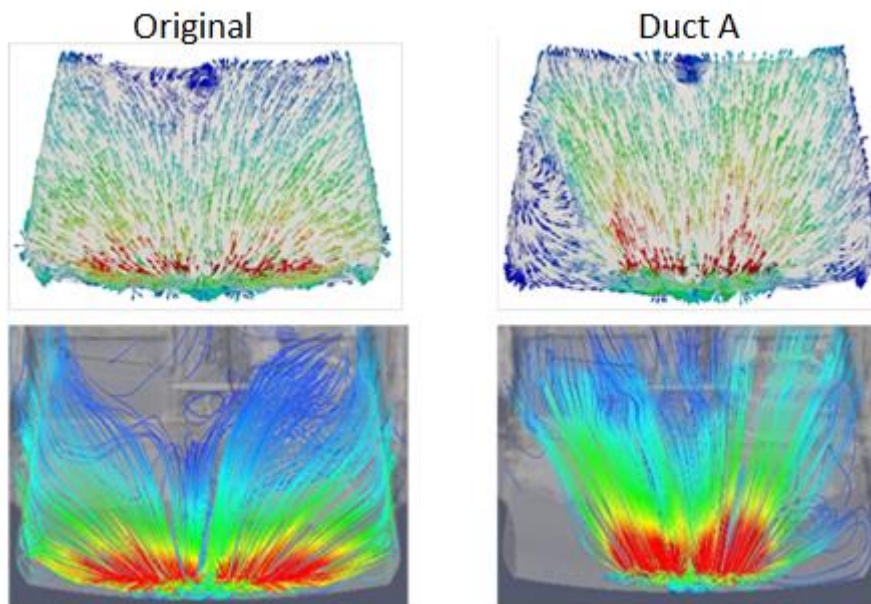


Figure 5.6: Streamlines of original duct and duct A

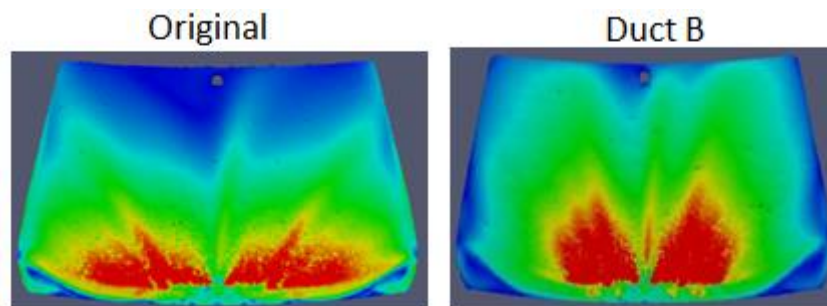


Figure 5.7: Velocity patterns of original duct and duct B

5.2 Objective Function

The target remains the same, to achieve velocities of minimum U_{tar} in order to get the appropriate level of defrosting and/or defogging. The used objective function is appropriate for the constant width duct since it leads to almost 0% of the upper windshield with a velocity lower than the target value set. Since the width is now an optimization variable due to the use of HUD, the current form of the objective function may be inappropriate. The reduced width in accordance to the same mass flow, results to high air velocity and a deficit appears at the base of the windshield and the sides.

As observed in Figure 5.8, the current objective function takes high values in areas where the velocity exceeds the minimum target, due to the fact that it evaluates the deviation from the target value. Although appropriate for studies where uniformity of the velocity pattern is a primary goal or in cases where the velocities in the optimization volume are consistently lower than the target value, it becomes evident that a new objective function should be used. This new objective function must penalize solutions with very low air velocity in both lower and upper parts of the windshield.

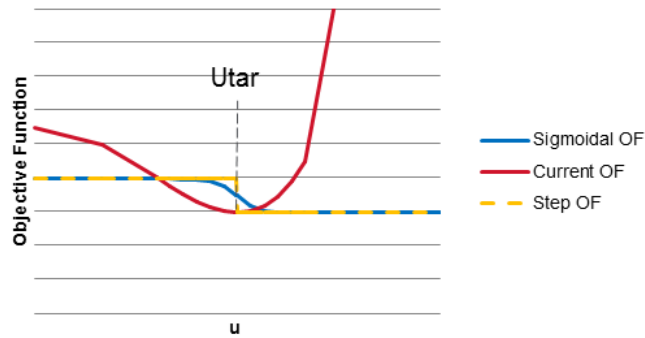


Figure 5.8: Current and proposed objective function

5.2.1 Definition of Objective Function

The new objective function is a sigmoid one which can be formulated as:

$$F_{obj} = \frac{1}{\Omega_{tar}} \int_{\Omega_{tar}} f_{obj} d\Omega_{tar}$$

$$f_{obj} = 1 - \frac{1}{1 + e^{-k_2(u - u_{min}) + k_1}}$$

$$k_1 = \ln\left(\frac{1}{e_{inf}} - 1\right)$$

$$k_2 = \frac{2k_1}{u_{max} - u_{min}}$$

5.1

e_{inf} : infinitesimally small positive number

The formulation of the sigmoid function instead of a simpler step function is made in order to ensure that the objective function can be differentiated and therefore, is appropriate for gradient-based optimization in future studies.

The equivalent step function is:

$$f_{obj}(u) = \begin{cases} 0, & u < u_{min} \\ 1, & u \geq u_{min} \end{cases} \quad 5.2$$

Although not used in this study, the derivative of the new objective function is presented below in order to be prepared for a future application of the adjoint method:

$$\begin{aligned} \frac{\partial F_{obj}}{\partial u} &= \frac{1}{\Omega_{tar}} \int_{\Omega_{tar}} \frac{\partial f_{obj}}{\partial u} d\Omega_{tar} \\ \frac{\partial f_{obj}}{\partial u} &= \frac{-k_2 e^{-k_2(u-u_{min})+k_1}}{(1 + e^{-k_2(u-u_{min})+k_1})^2} \end{aligned} \quad 5.3$$

The penalties assigned to each cell according to the sigmoid function are presented in the analysis below:

$$\begin{aligned} \text{For } u = u_{min}: \quad f_{obj} &= 1 - \frac{1}{1 + e^{-k_2(u_{min}-u_{min})+k_1}} = 1 - \frac{1}{1 + e^{k_1}} \\ \text{For } e_{inf} \rightarrow +0 &\Rightarrow \frac{1}{e_{inf}} \rightarrow +\infty \Rightarrow \frac{1}{e_{inf}} - 1 \rightarrow +\infty \Rightarrow \\ \ln\left(\frac{1}{e_{inf}} - 1\right) &\rightarrow +\infty \Rightarrow k_1 \rightarrow +\infty, \quad \text{since } k_1 = \ln\left(\frac{1}{e_{inf}} - 1\right) \end{aligned}$$

Therefore,

$$\begin{aligned} f_{obj} &= 1 - \frac{1}{1 + e^{k_1}} \\ k_1 \rightarrow +\infty &\Rightarrow \frac{1}{1 + e^{k_1}} \rightarrow +0 \Rightarrow 1 - \frac{1}{1 + e^{k_1}} \rightarrow 1 \Rightarrow f_{obj} \rightarrow 1 \end{aligned} \quad 5.4$$

$$\text{For } u = u_{max}: f_{obj} = 1 - \frac{1}{1 + e^{-k_2(u_{max}-u_{min})+k_1}}$$

$$k_1 = \ln\left(\frac{1}{e_{inf}} - 1\right)$$

$$k_2 = \frac{2k_1}{u_{max} - u_{min}}$$

Therefore,

$$\begin{aligned}
f_{obj} &= 1 - \frac{1}{1 + e^{-k_2(u_{max}-u_{min})+k_1}} = 1 - \frac{1}{1 + e^{-\frac{2k_1}{u_{max}-u_{min}}(u_{max}-u_{min})+k_1}} \\
&= 1 - \frac{1}{1 + e^{-k_1}}
\end{aligned} \tag{5.5}$$

Since $k_1 \rightarrow +\infty, e^{-k_1} \rightarrow +0, f_{obj} \rightarrow 0$

So, for $u < u_{min}$:

$$\begin{aligned}
u - u_{min} < 0 &\Leftrightarrow -2k_1 \frac{(u - u_{min})}{(u_{max} - u_{min})} \rightarrow +\infty \\
&\Leftrightarrow -k_2(u - u_{min}) + k_1 \rightarrow +\infty \\
&\Leftrightarrow -k_2(u - u_{min}) + k_1 \rightarrow +\infty \\
&\Leftrightarrow e^{-k_2(u - u_{min})+k_1} \rightarrow +\infty \\
&\Leftrightarrow 1 - \frac{1}{1 + e^{-k_2(u - u_{min})+k_1}} \rightarrow 1 \\
&\Leftrightarrow f_{obj} \rightarrow 1
\end{aligned} \tag{5.6}$$

and, for $u > u_{max}$:

$$\begin{aligned}
u - u_{min} > u_{max} - u_{min} > 0 \\
&\Leftrightarrow \frac{(u - u_{min})}{(u_{max} - u_{min})} > \frac{(u_{max} - u_{min})}{(u_{max} - u_{min})} = 1 \\
&\Leftrightarrow -\frac{2(u - u_{min})}{(u_{max} - u_{min})} < -2 \\
&\Leftrightarrow -\frac{2(u - u_{min})}{(u_{max} - u_{min})} + 1 < -1 \quad (1)
\end{aligned} \tag{5.7}$$

$$\begin{aligned}
-k_2(u - u_{min}) + k_1 &= \frac{-2k_1(u - u_{min})}{u_{max} - u_{min}} + k_1 = \\
&= k_1 \left(\frac{-2(u - u_{min})}{u_{max} - u_{min}} + 1 \right) \\
(1) \Rightarrow -\frac{2(u - u_{min})}{(u_{max} - u_{min})} + 1 < -1 < 0 &\Leftrightarrow k_1 \left(\frac{-2(u - u_{min})}{u_{max} - u_{min}} + 1 \right) \\
&\rightarrow -\infty \Leftrightarrow -k_2(u - u_{min}) + k_1 \rightarrow -\infty \Leftrightarrow f_{obj} \rightarrow 0
\end{aligned}$$

Summarizing, the penalties of the sigmoid function can be expressed as:

$$f_{obj}(u) \rightarrow \begin{cases} 1 - e_{inf} \cong +1, & u \leq u_{min} \\ e_{inf} \cong +0, & u \geq u_{max} \end{cases} \tag{5.8}$$

5.2.2 Error of Objective Function

The relative error of the objective function can be calculated by:

$$\begin{aligned}
error &= \frac{\varepsilon_{sig} - \varepsilon_{step}}{\varepsilon_{step}} \\
\varepsilon_{step} &= 1 \cdot u_{min} \\
\varepsilon_{sig} &= \int_0^{u_{min}} f_{obj} du + \int_{u_{min}}^{u_{max}} f_{obj} du + \int_{u_{max}}^{u_{\infty}} f_{obj} du \quad 5.9 \\
&\quad \uparrow \quad \quad \quad \uparrow \quad \quad \quad \uparrow \\
&\quad A \quad \quad \quad B \quad \quad \quad C
\end{aligned}$$

We assume that:

$$\begin{aligned}
A &= \int_0^{u_{min}} f_{obj} du = u_{min}(1 - e_{inf}) + (1 - 1 + e_{inf}) \frac{u_{min}}{2} = \\
&\quad = u_{min} \left(1 - \frac{e_{inf}}{2}\right) \\
C &= \frac{u_{\infty} - u_{max}}{2} e_{inf} \\
B &= \int_{u_{min}}^{u_{max}} f_{obj} du = \int_{u_{min}}^{u_{max}} \left(1 - \frac{1}{1 + e^{-k_2(u-u_{min})+k_1}}\right) du \quad 5.10 \\
&\quad = \int_{u_{min}}^{u_{max}} \left(\frac{e^{-k_2(u-u_{min})+k_1}}{1 + e^{-k_2(u-u_{min})+k_1}}\right) du \\
&\quad = -\frac{1}{k_2} [\ln 1 + e^{-k_2(u-u_{min})+k_1}]_{u_{min}}^{u_{max}} \\
&\quad = -\frac{1}{k_2} [\ln(1 + e^{-k_2(u_{max}-u_{min})+k_1}) - \ln(1 + e^{k_1})] \\
&\quad = -\frac{1}{k_2} [\ln(1 + e^{-k_1}) - \ln(1 + e^{k_1})] = -\frac{1}{k_2} \left[\ln\left(\frac{1 + e^{-k_1}}{1 + e^{k_1}}\right)\right] \\
&\quad = -\frac{1}{k_2} \ln \frac{1}{e^{k_1}} = \frac{k_1}{k_2} = \frac{k_1}{2k_1} (u_{max} - u_{min}) = \frac{1}{2} \left(\frac{u_{max}}{u_{min}} - 1\right) u_{min}
\end{aligned}$$

So, for $e_{inf} \approx 0$, $A \approx u_{min}$, $C \approx 0$, therefore,

$$\begin{aligned}
error &= \frac{\varepsilon_{sig} - \varepsilon_{step}}{\varepsilon_{step}} = \frac{u_{min} + \frac{1}{2} \left(\frac{u_{max}}{u_{min}} - 1\right) u_{min} - u_{min}}{u_{min}} \quad 5.11 \\
&\quad = \frac{1}{2} \left(\frac{u_{max}}{u_{min}} - 1\right) = \frac{100}{2} \left(\frac{u_{max}}{u_{min}} - 1\right) \%
\end{aligned}$$

5.3 Results of Study

Having selected the ducts of width A and B, we proceed with the DoE study in order to establish which geometry is most promising, the same procedure as in the previous chapter is followed.

In both width A and B cases we have: $3^3+2^3=35$ geometries. The first $3^3=27$ geometries have the same parameters as shown in Table 4.2 and the parameters of the remaining $2^3=8$ geometries are shown in Table 4.3.

The performance of the original, width A and width B geometries are depicted in Figure 5.9. For the studied geometries, the error value (Eq. 5.11) was found to be below 2%.

Indicatively, the performance for 3 of 35 ducts along with their geometry for width A, are depicted in Figure 5.10 while Table 5.1 shows the percentage difference of the objective function between those 3 ducts and the original one.

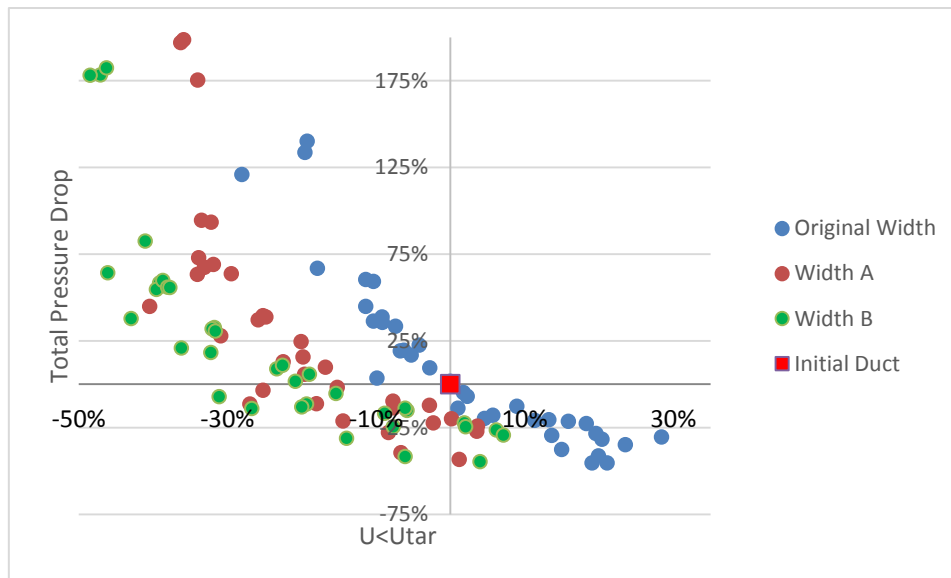


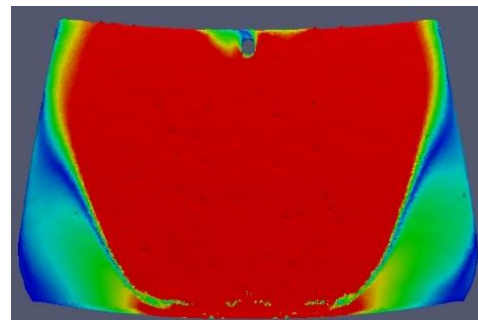
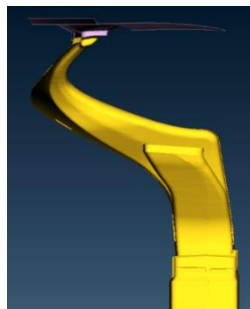
Figure 5.9: Performance of the original, width A and width B geometries

D: Distance
O: Opening
A: Angle

Duct appearance

Duct performance

D: Min
O: Min
A: Min



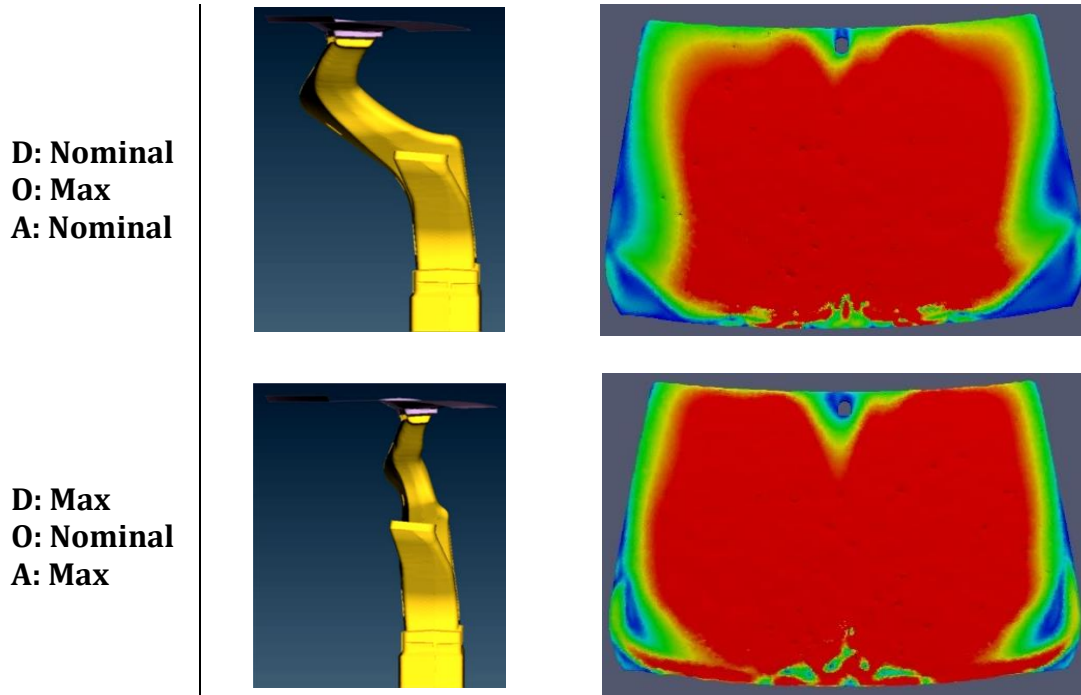


Figure 5.10: Geometry and performance of various width A ducts

Table 5.1: Objective function difference of various width A ducts

Duct	Obj. Function difference [%]
D: Min, O: Min, A: Min	-35.9
D: Nom., O: Max, A: Nom.	-2.3
D: Max, O: Nom, A: Max	-26.9

Having examined the results of the DoE studies, we conclude that for both width A and B cases, the most promising geometries have the same parameter values. The parameter values and the objective function and total pressure drop percentage difference are presented in Table 5.2 whereas the duct performance and geometry can be seen in Figure 5.11.

Table 5.2: Objective function and total pressure drop difference of optimal ducts

Width	Design Parameters	Objective Function	Total pressure Drop
A	D: Max O: Nom A: Max	-26.9%	-11.5%
B		-26.7%	-14.1%

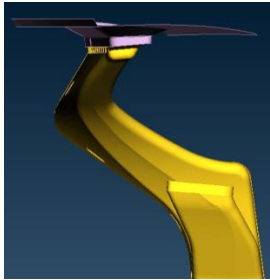
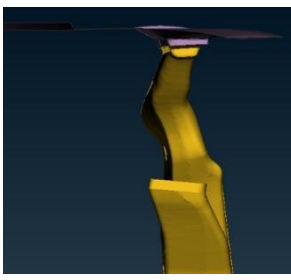
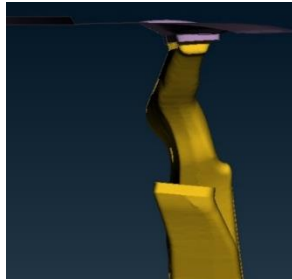
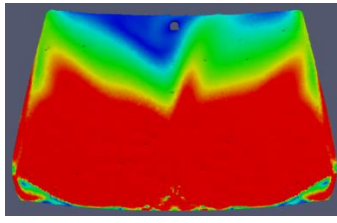
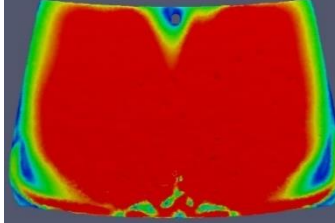
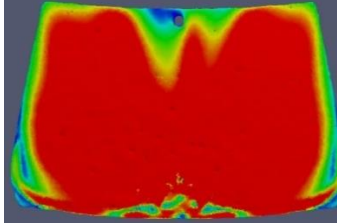
Parameter Values	<u>Original Duct</u>	<u>Duct Width A</u>	<u>Duct Width B</u>
Geometry			
Duct Performance			

Figure 5.11: Geometry and performance of most promising width A and B ducts

5.4 Operation for different mass flows

The reduced width ducts were further studied concerning their performance for varied mass flow. Indicatively, the comparison of performance between the original and the reduced width A duct for various mass flow percentages, is depicted in Figure 5.12. As it can be seen, even for low mass flow values, the reduced width duct (compared to the original) has higher stream velocities which result to sufficient defogging and defrosting.

This performance indicates that the reduced width ducts can operate in the appropriate manner even using lower power. In this way, these ducts can be used in cars where low power consumption is mandatory (i.e. hybrids). Thus, the manufacturing line of the HVAC could be the same for different vehicles changing only the programming for the flow value for power reduction.

It should be noted that higher mass flow will defog/defrost the windshield more quickly than lower mass flow. Thus, in order to find the most efficient

concept, the time needed and the power consumption for various mass flows should be considered. The above can result to a duct geometry that can be used into different cars and having different mass flow and power consumption according to its programming.

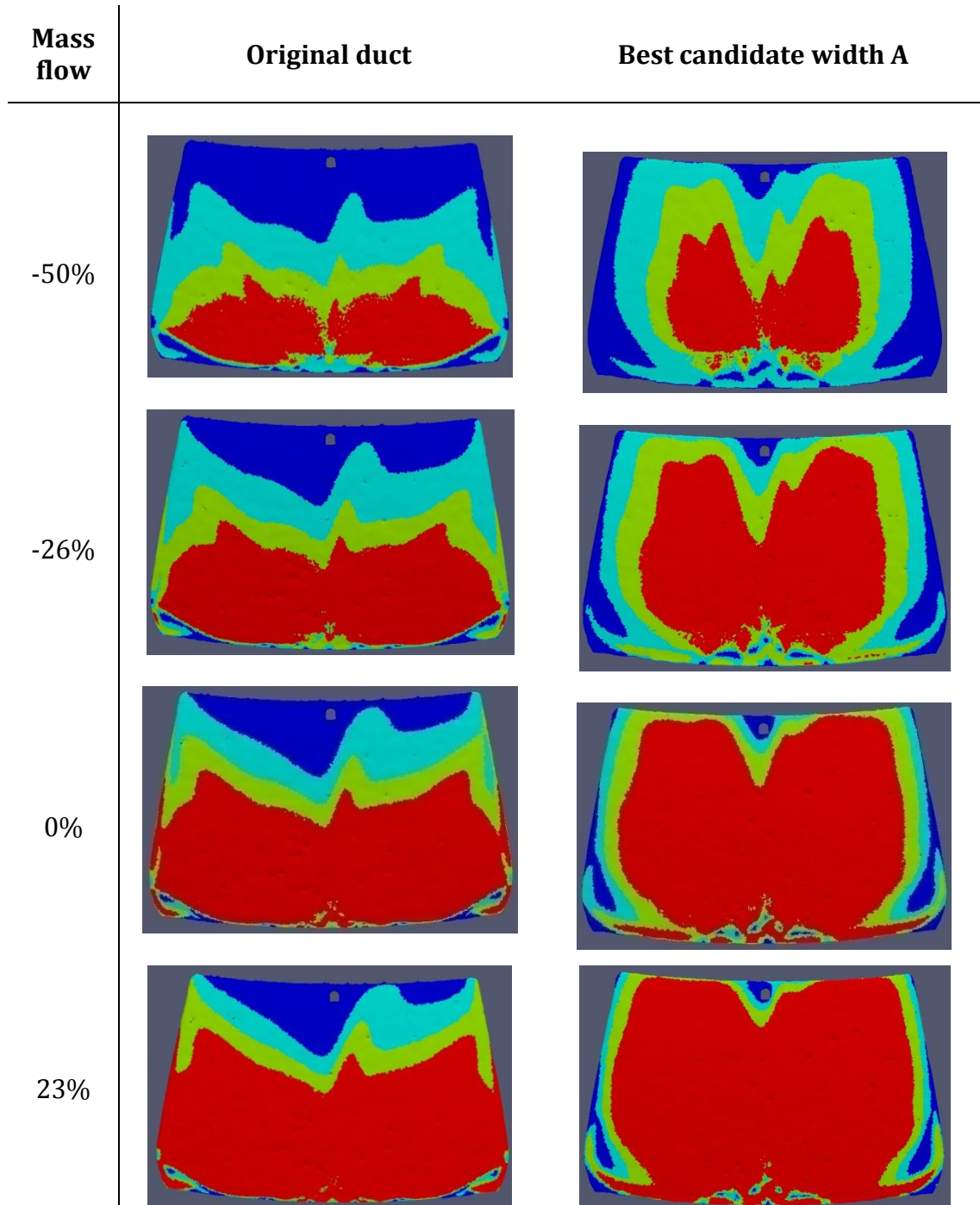


Figure 5.12: Performance of original and width A duct for various mass flows

6 Conclusions and Future Research

6.1 Conclusions

Aim of this work was to optimize the HVAC duct geometry of a TOYOTA Yaris passenger car for better performance. The optimal geometry is derived by optimization process which is based on a metamodel-assisted evolutionary algorithm (MAEA). This geometry can be used as the starting point for the adjoint optimization method for fine tuning and for reaching the global optimum solution. With this procedure, an optimized geometry was found which has 22% lower value of the objective function and the same total pressure drop with the original one.

Due to the possibility of installing a HUD device, a preliminary study concerning the width of the duct was carried out. Since the width is now an optimization variable due to the use of HUD, a new objective function was developed and used which will penalize solutions with very high or very low air velocity. It was found that, as the width decreases, there is: a) improvement of velocity pattern in upper half windshield, b) loss of velocity on lower sides of windshield and c) increase of total pressure drop. Further optimization can be carried out when the geometry of the HUD device is known.

6.2 Future Research

From the findings of this work and the nature of the studied problem, the further research steps that propose are:

- Concerning the original duct, the optimized geometry that it was found should be used as a starting point for an adjoint optimization in order to fine tune the already available solutions.
- Concerning the new duct and when the HUD geometry is known, the findings of the DoE study can be used in a MAEA optimization procedure to find the optimal geometry which can then be used as a starting point for the adjoint optimization.

Bibliography

- L. Germanou, E.M. Papoutsis-Kiachagias, A. Delacroix, and K.C. Giannakoglou, "Defroster nozzle shape optimization using the continuous adjoint method", ECCOMAS Congress 2016, VII European Congress on Computational Methods in Applied Sciences and Engineering, Crete island, Greece, June 5-10, 2016 .
- M. Ablassmeier, T. Poitschke, F. Wallhoff, K. Bengler and G. Rigoll, "Eye Gaze Studies Comparing Head-Up and Head-Down Displays in Vehicles," 2007 IEEE International Conference on Multimedia and Expo, Beijing, 2007, pp. 2250-2252, doi: 10.1109/ICME.2007.4285134
- J. Antony, 2003, "Design of Experiments for Engineers and Scientists", Elsevier, ISBN 978-0-7506-4709-0, doi: 10.1016/B978-0-7506-4709-0.X5000-5
- G. Burnett, 2003, "A road-based evaluation of a Head-Up Display for presenting navigation information", Proceedings of HCI International conference, Vol 3 (Human-Centered Computing), pp. 180-184, Crete, Greece, June 23-27, 2003
- M. Cavazzuti, 2013, "Optimization Methods From Theory to Design Scientific and Technological Aspects in Mechanics", Springer, ISBN 978-3-642-31186-4, doi: 10.1007/978-3-642-31187-1
- V. Charissis, S. Papanastasiou, G. Vlachos, 2008, "Comparative Study of Prototype Automotive HUD vs. HDD: Collision Avoidance Simulation and Results", doi: 10.4271/2008-01-0203.
- W. Horrey, C. Wickens, 2004, "Driving and Side Task Performance: The Effects of Display Clutter, Separation, and Modality", Human Factors: The Journal of the Human Factors and Ergonomics Society, doi: 10.1518/hfes.46.4.611.56805
- I.C. Karpolis, K.C. Giannakoglou, 2009, "Distributed Evolutionary Algorithms with Hierarchical Evaluation", Engineering Optimization - ENG OPTIMIZ. 41. 1037-1049. doi: 10.1080/03052150902890072.
- I.C. Karpolis, A.S. Zymaris, V.G. Asouti, K.C. Giannakoglou, "Multilevel optimization strategies based on metamodel-assisted evolutionary algorithms, for computationally expensive problems," 2007 IEEE Congress on Evolutionary Computation, Singapore, 2007, pp. 4116-4123, doi: 10.1109/CEC.2007.4425008
- Y.C. Liu, "Effects of using head-up display in automobile context on attention demand and driving performance", Displays, Volume 24, Issues 4-5, 2003, ISSN 0141-9382, doi: 10.1016/j.displa.2004.01.001

- Y.C. Liu, M.H. Wen, "Comparison of head-up display (HUD) vs. head-down display (HDD): driving performance of commercial vehicle operators in Taiwan", *International Journal of Human-Computer Studies*, Volume 61, Issue 5, 2004, ISSN 1071-5819, doi: 10.1016/j.ijhcs.2004.06.002
- J. Park, C. Kim, 2003, "Parametric Study on Automotive Windshield Defrost Pattern using CFD", doi: 10.4271/2003-01-1078.
- C. Rao, H. Toutenburg, Shalabh, C. Heumann, 2008, "Linear Models and Generalizations, Least Squares and Alternatives", Springer, ISBN 978-3-540-74226-5, doi: 10.1007/978-3-540-74227-2
- M. Shojaeefard, G. Molaeimasli, N. Aghamirzaei, S. Ghezelbiglo, B. Zeinolabedini, 2015, "Numerical evaluation of the defrosting/defogging performance of HVAC system in the main product of the national vehicle platform", *International Journal of Automotive Engineering*, Vol. 5, Number 4, Dec 2015
- R. Sojourner, J. Antin, 1990, "The effects of a simulated head-up display speedometer on perceptual task performance", *Human Factors The Journal of the Human Factors and Ergonomics Society*, doi: 10.1177/001872089003200306
- S. Sugarman, 2005, "HVAC Fundamentals", The Fairmont Press, Inc., ISBN 088173490X, 9780881734904
- K.C. Giannakoglou, 2005, "Optimization methods in aerodynamics", NTUA In Greek "Μέθοδοι Βελτιστοποίησης στην Αεροδυναμική", Εκδόσεις ΕΜΠ
- E.M. Papoutsis-Kiachagias, S.A. Kyriacou, K.C. Giannakoglou, "The Continuous Adjoint Method for the Design of Hydraulic Turbomachines", *Computer Methods in Applied Mechanics and Engineering* 2014; 278:621-639
- D.C. Montgomery, "Design and Analysis of Experiments", ISBN-13: 978-1118146927
- S.A. Kyriacou, V.G. Asouti, K.C. Giannakoglou, "Efficient PCA-driven EAs and metamodel-assisted EAs, with applications in turbomachinery", *Engineering Optimization* 2014; 46(7):895-911
- M. Karakasis, K.C. Giannakoglou, "On the Use of Metamodel-Assisted Multi-Objective Evolutionary Algorithms", *Engineering Optimization* 2006; 38(8):941-957
- V.G. Asouti, I.C. Kambolis, K.C. Giannakoglou, "A grid-enabled asynchronous metamodel-assisted evolutionary algorithm for aerodynamic optimization", *Genetic Programming and Evolvable Machines (SI:Parallel and Distributed Evolutionary Algorithms, Part One)*, 10(3):373-389, 2009.
- E.A. Kontoleonos, V.G. Asouti, K.C. Giannakoglou, "An asynchronous metamodel-assisted memetic algorithm for cfd-based shape optimization", *Engineering Optimization*, 44(2):157-173, 2012.

- W.G. Cochran, G.M. Cox, 1957, "Experimental Design", 2nd edition
- K.C. Giannakoglou, A.P. Giotis, M.K. Karakasis, 2001, "Low-cost genetic optimization based on inexact pre-evaluations and the sensitivity analysis of design parameters", *Inverse Problems in Engineering*, 9:4, 389-412, doi: 10.1080/174159701088027771
- N. Marco, S. Lanteri, 2000, "A two-level parallelization strategy for Genetic Algorithms applied to optimum shape design", *Parallel Computing* 26 377-397
- K.C. Giannakoglou, 2002, "Design of optimal aerodynamic shapes using stochastic optimization methods and computational intelligence", *Progress in Aerospace Sciences* 38 43-76
- K.C. Giannakoglou, D.I. Papadimitriou, I.C. Kampolis, 2006, "Aerodynamic shape design using evolutionary algorithms and new gradient-assisted metamodels", *Comput. Methods Appl. Mech. Engrg.* 195 6312-6329
- H. K. Versteeg, W. Malalasekera, 1995, "An introduction to computational fluid dynamics. The Finite volume method"
- J. Nocedal, S. J. Wright, 1999, "Numerical Optimization", Springer
- E.M. Papoutsis-Kiachagias, A.S. Zymaris, I.S. Kavvadias, D.I. Papadimitriou, K.C. Giannakoglou, 2015, "The continuous adjoint approach to the $k-\epsilon$ Turbulence model for shape optimization and optimal active control of turbulent flows", *Engineering Optimization*, 47 (3), pp. 370-389

Εκτενής Περίληψη Διπλωματικής Εργασίας:
Βελτιστοποίηση Γεωμετρίας Αεραγωγού
Αυτοκινήτου



ΕΘΝΙΚΟ ΜΕΤΣΟΒΙΟ ΠΟΛΥΤΕΧΝΕΙΟ
ΣΧΟΛΗ ΜΗΧΑΝΟΛΟΓΩΝ ΜΗΧΑΝΙΚΩΝ
ΤΟΜΕΑΣ ΡΕΥΣΤΩΝ
ΜΟΝΑΔΑ ΠΑΡΑΛΛΗΛΗΣ ΥΠΟΛΟΓΙΣΤΙΚΗΣ
ΡΕΥΣΤΟΔΥΝΑΜΙΚΗΣ & ΒΕΛΤΙΣΤΟΠΟΙΗΣΗΣ

Βελτιστοποίηση Γεωμετρίας Αεραγωγού **Αυτοκινήτου**

Διπλωματική Εργασία
Μαριάννα Παναγιωτίδου

Επίβλεψη:
Καθηγητής Κ. Χ. Γιαννάκογλου

Αθήνα
Φεβρουάριος 2019

Στόχος Διπλωματικής Εργασίας

Στόχος της διπλωματικής εργασίας είναι η εφαρμογή μεθόδων Σχεδιασμού Πειραμάτων και στοχαστικών μεθόδων βελτιστοποίησης, στον αγωγό αποπαγοποίησης του μπροστινού ανεμοθώρακα (παρμπρίζ) ενός αυτοκινήτου Toyota Yaris. Σκοπός της διαδικασίας βελτιστοποίησης είναι η επίτευξη βελτιωμένης απόδοσης και αποθάμβωσης για το όχημα. Επιπλέον, μελετάται η επίδραση του πλάτους του αγωγού προκειμένου να βρεθεί μια κατάλληλη γεωμετρία για την περίπτωση εγκατάστασης συστήματος διαφανούς οθόνης δεδομένων στο παρμπρίζ (Head-Up Display, HUD).

Αυτή η διπλωματική εργασία ενσωματώνει σχεδιασμό τεχνικών πειραμάτων, μορφοποίηση πλέγματος, μοντέλα παλινδρόμησης και εξελικτικούς αλγορίθμους. Αναπτύσσεται επίσης μια νέα αντικειμενική συνάρτηση που είναι πιο αντιπροσωπευτική του στόχου της αύξησης της αποπάγωσης και, επομένως, περισσότερο κατάλληλη για την υπόψη μελέτη.

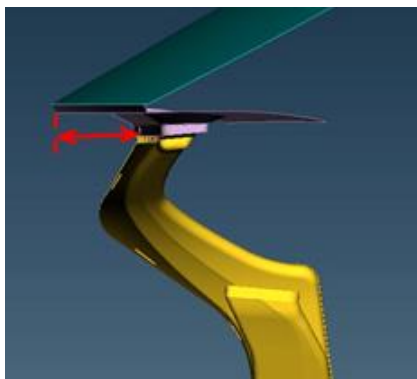
Βελτιστοποίηση του Αρχικού Αγωγού

Καθορισμός Παραμέτρων Μελέτης Σχεδιασμού Πειραμάτων

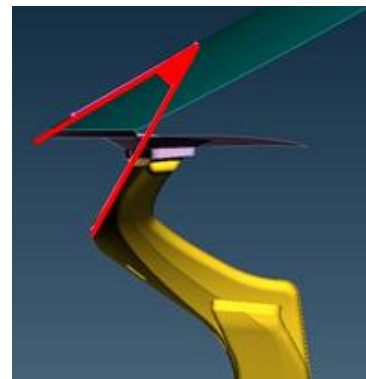
Ορίζονται αρχικά οι παράμετροι σχεδιασμού και το εύρος τους:

1. Απόσταση: η απόσταση της εξόδου του αγωγού από τη βάση του ανεμοθώρακα (Σχήμα 1)
2. Γωνία: η γωνία μεταξύ της εξόδου του αγωγού και της εφαπτομένης στο κέντρο του παρμπρίζ (Σχήμα 2)
3. Άνοιγμα: το πλάτος της εξόδου του αγωγού (Σχήμα 3)

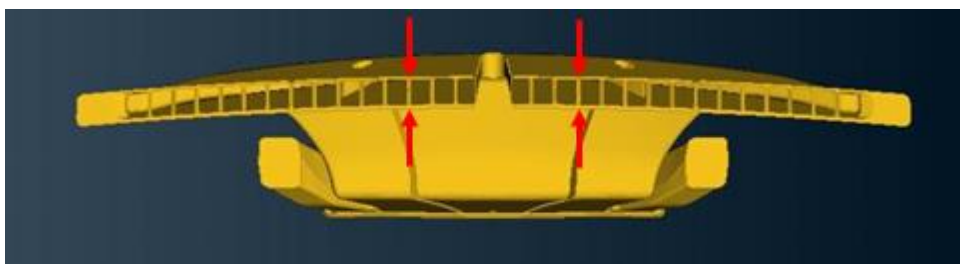
Προτείνεται ένας σχεδιασμός τριών επιπέδων προκειμένου να μοντελοποιηθεί η τυχόν καμπυλότητα της συνάρτησης απόκρισης και να διαχειριστούν οι ονομαστικοί παράγοντες σε 3 επίπεδα. Με τρεις μεταβλητές σχεδιασμού [k] και έναν πλήρη παραγοντικό σχεδιασμό τριών επιπέδων (3^k παραγοντικός σχεδιασμός) προκύπτουν $3^3=27$ νέες γεωμετρίες άρα και 27 προσομοιώσεις για να καθοριστεί η απόδοση των υποψήφιων γεωμετριών.



Σχήμα 1: Παράμετρος Σχεδιασμού: Απόσταση



Σχήμα 2: Παράμετρος Σχεδιασμού: Γωνία

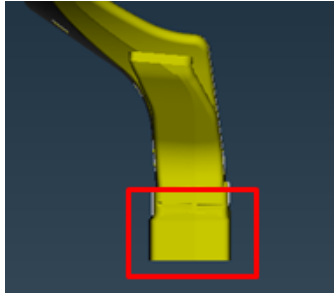


Σχήμα 3: Παράμετρος Σχεδιασμού: Άνοιγμα

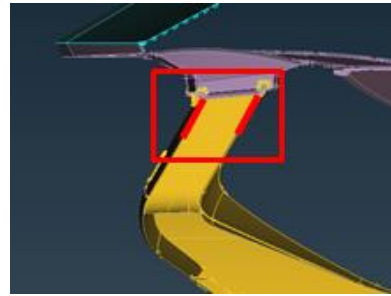
Έχοντας επιλέξει τις παραμέτρους σχεδιασμού, καθορίζονται κατάλληλοι περιορισμοί έτσι ώστε να επιτευχθούν επιθυμητές και ρεαλιστικές γεωμετρίες. Στη μελέτη αυτή, οι περιορισμοί κατατάσσονται σε 2 κατηγορίες:

α. γεωμετρικοί περιορισμοί λόγω προδιαγραφών σχετικών μεταξύ άλλων με την κατασκευή, τη λειτουργικότητα και την αισθητική του αγωγού και του πίνακα οργάνων (Σχήμα 4, Σχήμα 5, Σχήμα 6)

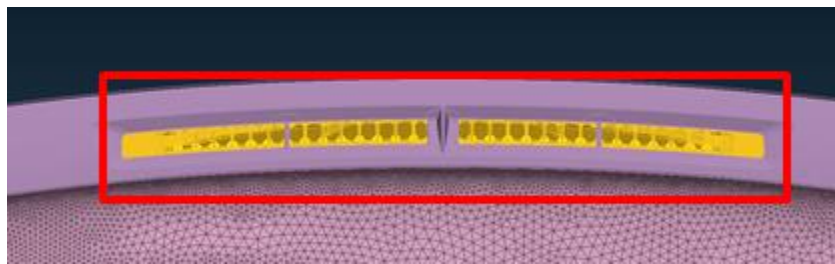
β. περιορισμοί σχετικοί με την πτώση ολικής πίεσης για να επιτευχθεί βέλτιστη απόδοση διατηρώντας χαμηλά τα επίπεδα της κατανάλωσης ισχύος.



Σχήμα 4: Περιορισμός 1: Καθορισμένη θέση και σχήμα της εισόδου του αγωγού



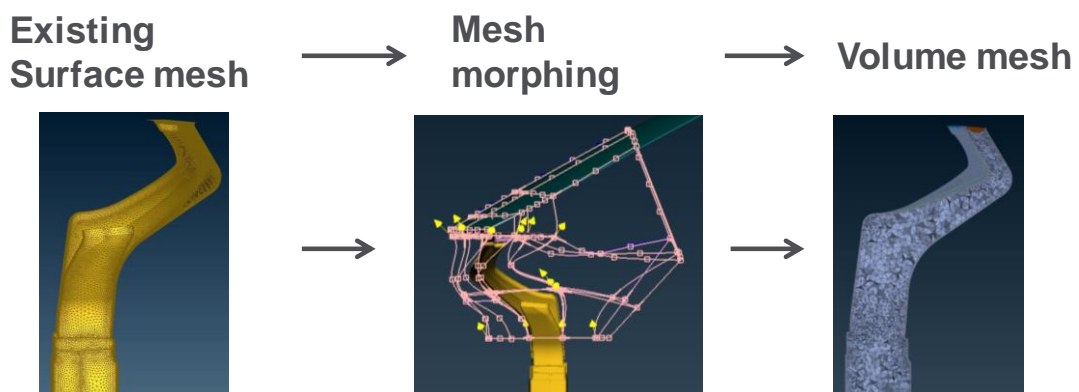
Σχήμα 5: Περιορισμός 2: Παράλληλα τοιχώματα της εξόδου του αγωγού



Σχήμα 6: Περιορισμός 3: Σταθερή απόσταση από το παρμπρίζ και πλάτος ανοίγματος της εξόδου του αγωγού καθ' όλο το μήκος του αγωγού

Προετοιμασία Νέων Γεωμετριών

Οι 27 νέες γεωμετρίες που έχουν προκύψει από τον παραγοντικό σχεδιασμό μοντελοποιούνται στον υπολογιστή κάνοντας χρήση εργαλείων μορφοποίησης επιφανειακού πλέγματος (Σχήμα 7).

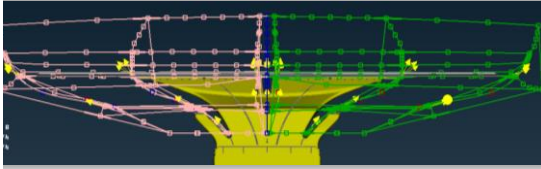


Σχήμα 7: Μοντελοποίηση γεωμετριών με μορφοποίηση πλέγματος

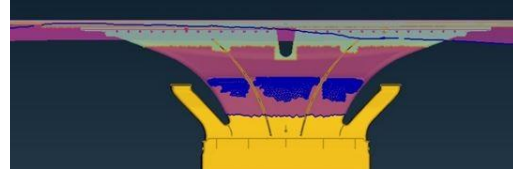
Τα διαθέσιμα εργαλεία μορφοποίησης που χρησιμοποιούνται είναι δύο:

- a. Παράμετρος γωνίας: μορφοποίηση χωρίου, τα στοιχεία που βρίσκονται εντός του χωρίου μορφοποιούνται με μετακίνηση ή κύλιση των σημείων ελέγχου που βρίσκονται στις ακμές του χωρίου (Σχήμα 8).

- b. Παράμετρος απόστασης και ανοίγματος: μορφοποίηση απευθείας εφαρμογής, το επιλεγμένο τμήμα του μοντέλου μετακινείται ως μη παραμορφώσιμο σώμα και οι περιβάλλουσες περιοχές απορροφούν τη μετατόπιση χωρίς να προκαλέσουν ασυνέχειες στο μοντέλο (Σχήμα 9).



Σχήμα 8: Μορφοποίηση χωρίου



Σχήμα 9: Μορφοποίηση Απευθείας Εφαρμογής

Επίλυση

Έχοντας γενέσει τα νέα πλέγματα και ορίσει τις οριακές συνθήκες, η λύση της ροής προκύπτει επιλύοντας τις Reynolds-Averaged Navier–Stokes (RANS) εξισώσεις υποθέτοντας ότι η ροή είναι σταθερή στο χρόνο. Η ροή θεωρείται ασυμπίεστη και υιοθετείται το μοντέλο τύρβης k-ε. Τέλος, επιλέγεται ακρίβεια 2^{ης} τάξης.

Στόχοι και Αντικειμενική Συνάρτηση

Στόχοι της βελτιστοποίησης είναι η επίτευξη ομοιόμορφης κατανομής ταχυτήτων άνω της U_{tar} μπροστά από τον ανεμοθώρακα καθώς και η αποφυγή αύξησης της ολικής πίεσης p_t μεταξύ εισόδου και εξόδου του αγωγού.

Η αξιολόγηση κάθε νέου σχήματος πραγματοποιείται με τη χρήση της αντικειμενικής που εκφράζει την απόκλιση των ταχυτήτων από την επιθυμητή:

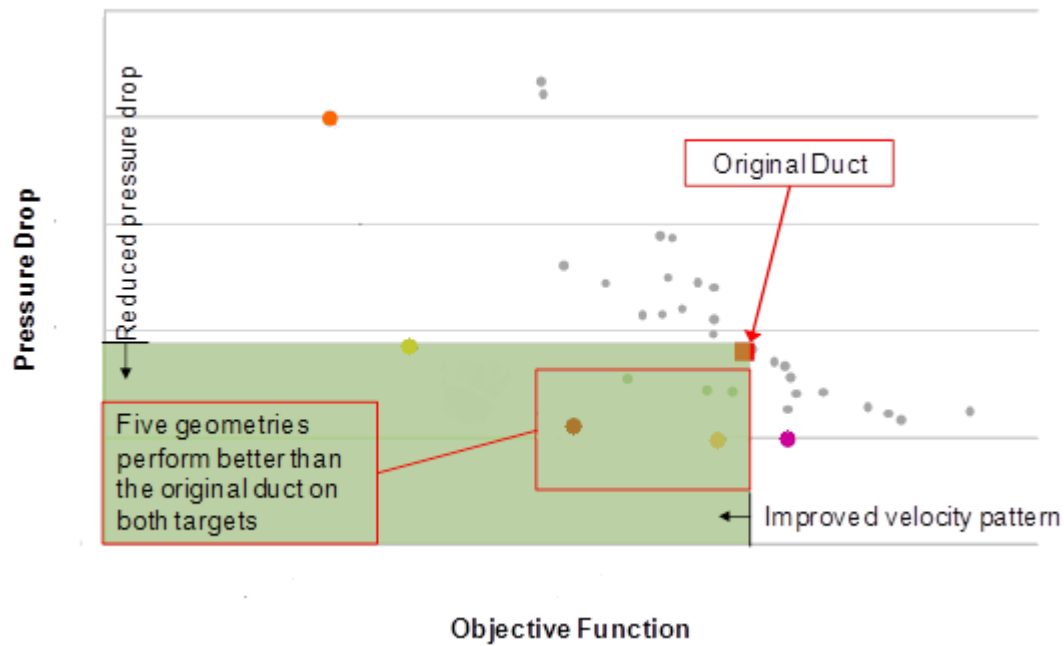
$$F_{obj} = \frac{1}{2} \int_{\Omega_{tar}} (u_i^2 - u_{i,tar}^2)^2 d\Omega_{tar}$$

όπου Ω_{tar} είναι ένας μικρός όγκος ελέγχου μπροστά από το παρμπρίζ.

Όγκος ελέγχου ορίζεται το άνω μισό τμήμα μπροστά από το παρμπρίζ καθώς στο κάτω τμήμα οι ταχύτητες είναι ως επί το πλείστον πάνω από 5m/s, και επομένως, συνεισφέρουν στην αύξηση της τιμής της αντικειμενικής χωρίς να αποτελεί πραγματικά το τμήμα αυτό προβληματική περιοχή.

Αποτελέσματα μελέτης Σχεδιασμού Πειραμάτων

Εξετάζοντας την απόδοση των 27 αγωγών συμπεραίνεται ότι οι μεταβλητές Απόσταση και Άνοιγμα έχουν σημαντική επίδραση στην αντικειμενική συνάρτηση (F_{obj}) και στην πτώση ολικής πίεσης (p_t) υψηλότερες τιμές απόστασης έχουν ως αποτέλεσμα χαμηλότερες τιμές F_{obj} και p_t , υψηλότερες τιμές διανοίγματος έχουν ως αποτέλεσμα υψηλότερες τιμές F_{obj} αλλά και χαμηλότερες τιμές p_t . Τέλος, η γωνία έχει μικρή επίδραση τόσο στην F_{obj} όσο και στην p_t . Η απόδοση των 27 γεωμετριών όσον αφορά την απόκλιση της ταχύτητας από την επιθυμητή και την πτώση ολικής πίεσης παρουσιάζονται στο Σχήμα 10.



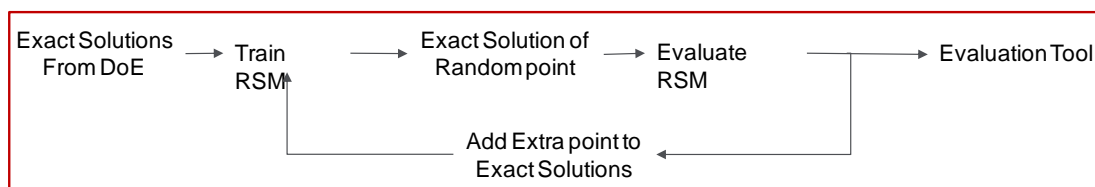
Σχήμα 10: Απόδοση των 27 γεωμετριών

Βελτιστοποίηση με Εξελικτικό Αλγόριθμο

Η επίλυση της ροής και κατ' επέκταση ο υπολογισμός της απόδοσης του αγωγού με επίλυση των RANS εξισώσεων συνεπάγεται υψηλό υπολογιστικό κόστος, για να αντιμετωπιστεί το πρόβλημα αυτό, υιοθετείται ως εργαλείο αξιολόγησης του εξελικτικού αλγορίθμου ένα μοντέλο παλινδρόμησης που προσεγγίζει τις ακριβές (τόσο ποιοτικά όσο και από άποψη κόστους) τιμές της αντικειμενικής συνάρτησης. Η μαθηματική έκφραση του μοντέλου παλινδρόμησης είναι:

$$y = \sum_{i=1}^3 a_{3i}x_i + \sum_{i=1}^3 a_{3i-1}x_i^2 + \sum_{i=3}^3 a_{3i-2}x_i^3 + \sum_{i=1}^3 \sum_{\substack{j=2 \\ i < j}}^3 a_{i+(j-2)+9}x_i x_j$$

Η διαδικασία εκπαίδευσης του νέου εργαλείου αξιολόγησης απεικονίζεται στην Σχήμα 11.

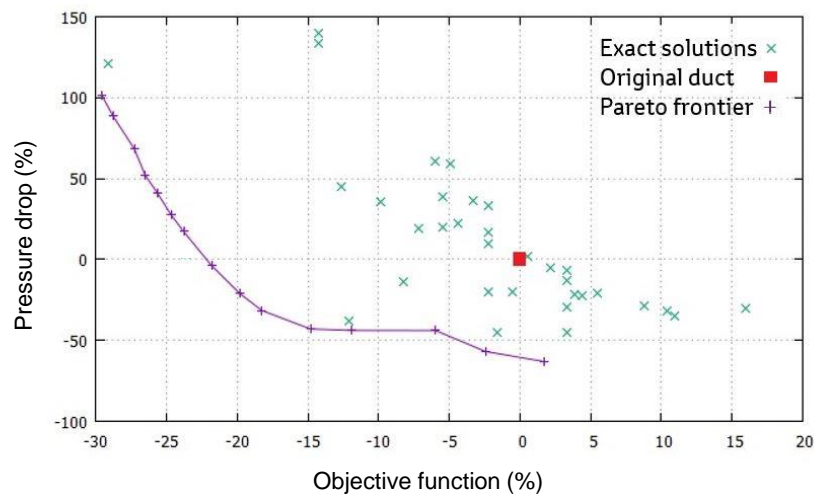


Σχήμα 11: Διαδικασία εκπαίδευσης λογισμικού αξιολόγησης

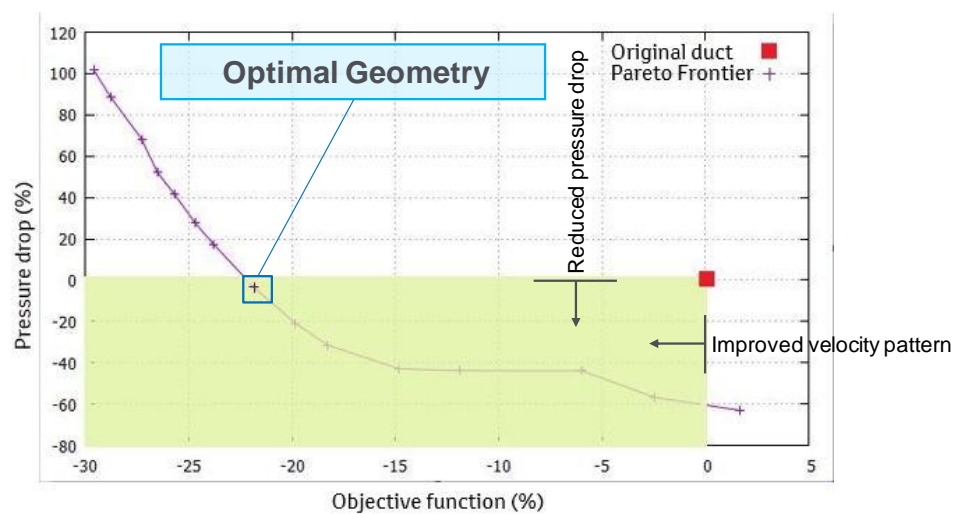
Χρησιμοποιείται το λογισμικό γενικής βελτιστοποίησης EASY v2.0. Ας σημειωθεί ότι εφαρμόστηκε ένας (30,90)EA και το προαναφερθέν αποσυνδεδεμένο μεταπρότυπο για την αξιολόγηση των λύσεων.

Αποτελέσματα βελτιστοποίησης

Παρατηρείται ότι υπάρχουν πολλές γεωμετρίες που έχουν καλύτερη απόδοση από τον αρχικό αγωγό (Σχήμα 12). Η βέλτιστη γεωμετρία θα προκύψει από επιλογή σημείου πάνω στο Pareto με κριτήριο την σχέση ανάμεσα σε πτώση p_t και F_{obj} . Προκειμένου να μην μεταβληθεί το φορτίο στον ανεμιστήρα της μονάδας κλιματισμού, η πτώση p_t πρέπει να διατηρεί σταθερή τιμή, ίση με αυτή του αρχικού αγωγού, επομένως η βέλτιστη γεωμετρία πρέπει να έχει μηδενική ποσοστιαία μεταβολή. Με βάση τα παραπάνω επιλέγεται η βέλτιστη γεωμετρία αγωγού (Σχήμα 13) που έχει τόση p_t όση και του αρχικού αγωγού και μειωμένη τιμή της F_{obj} κατά 22% σε σχέση με τον αρχικό αγωγό.


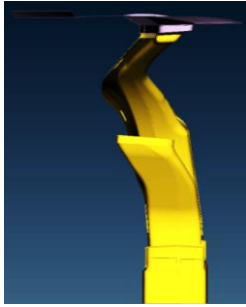


Σχήμα 12: Υπολογισθέν Μέτωπο Pareto EA

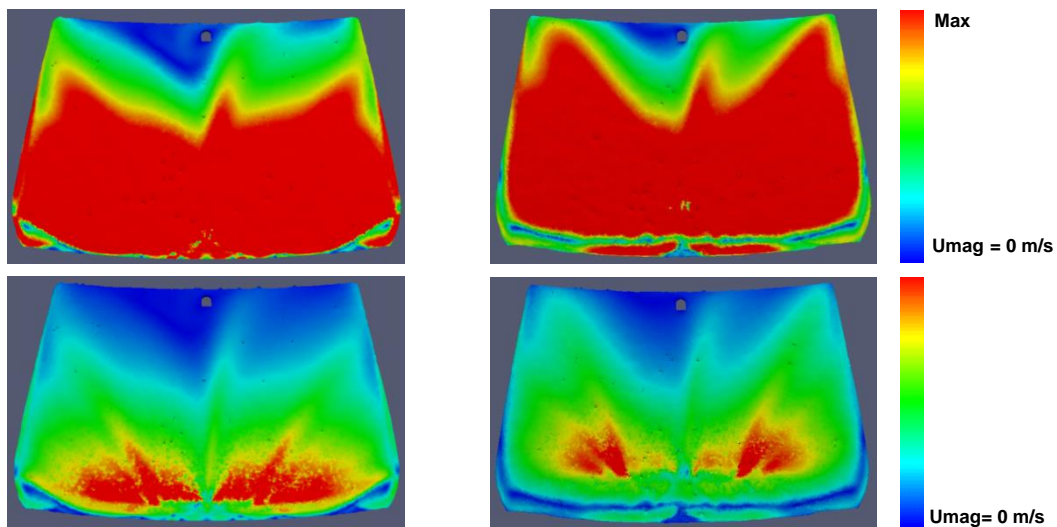


Σχήμα 13: Επιλογή βέλτιστης λύσης

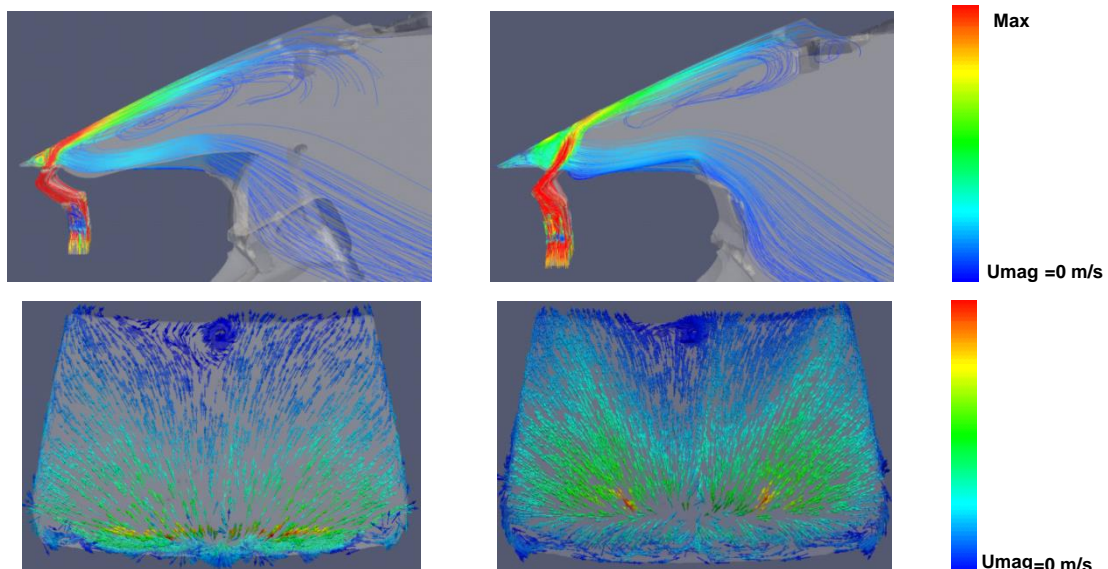
Παρουσιάζεται παρακάτω η γεωμετρία και η απόδοση του αρχικού και βέλτιστου αγωγού:

	Original Duct	Optimal Duct
		
Distance	-	240%
Opening	-	8%
Angle	-	-35%
F_{obj}	-	22%
p_t	-	-7%

Σχήμα 14: Αρχικός και βέλτιστος αγωγός



Σχήμα 15: Ταχύτητες αρχικού (αριστερά) και βέλτιστου αγωγού (δεξιά) πλησίον του ανεμοθώρακα



Σχήμα 16: Ροϊκές γραμμές και διανύσματα ταχυτήτων αρχικού και βέλτιστου αγωγού

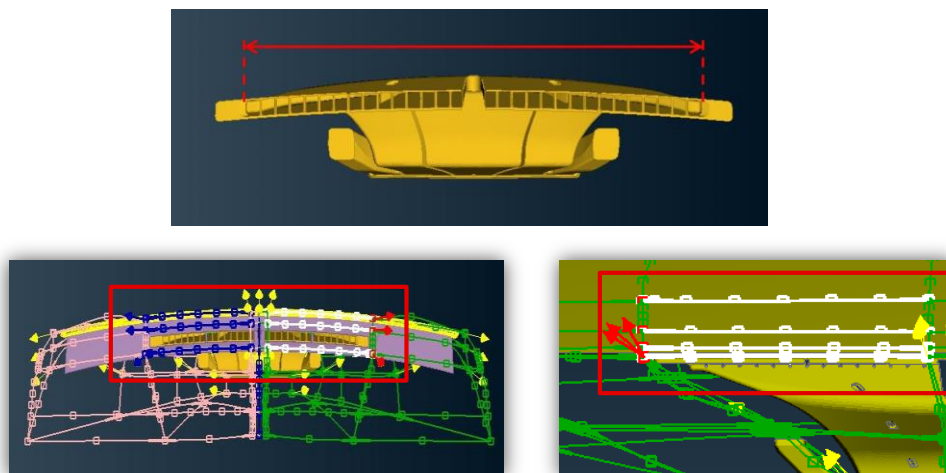
Μελέτη Μείωσης Πλάτους

Εξήγηση της παραμέτρου Πλάτους

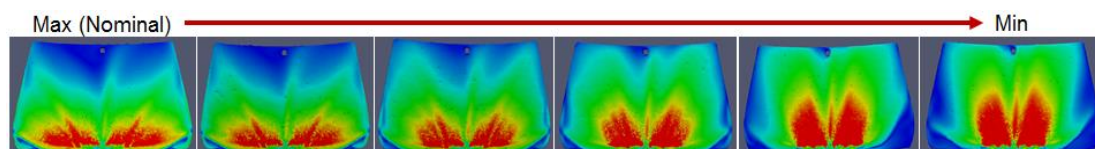
Μελλοντικές εγκαταστάσεις συστήματος διαφανούς οθόνης δεδομένων στον ανεμοθώρακα (Head-Up Display, HUD) στα νέα αυτοκίνητα απαιτούν μείωση του πλάτους του αγωγού προκειμένου να ελευθερωθεί χώρος για την άνετη εφαρμογή της οθόνης. Παρουσιάζεται μία παραμετρική μελέτη, στην οποία μεταβάλλεται το πλάτος του αγωγού, για να καθοριστεί η επίδραση στην απόδοση. Για τις πιο πολλά υποσχόμενες γεωμετρίες που θα προκύψουν, θα πραγματοποιηθεί μελέτη Σχεδιασμού Πειραμάτων, όπως στην περίπτωση ονομαστικού πλάτους.

Παραμετρική Μελέτη

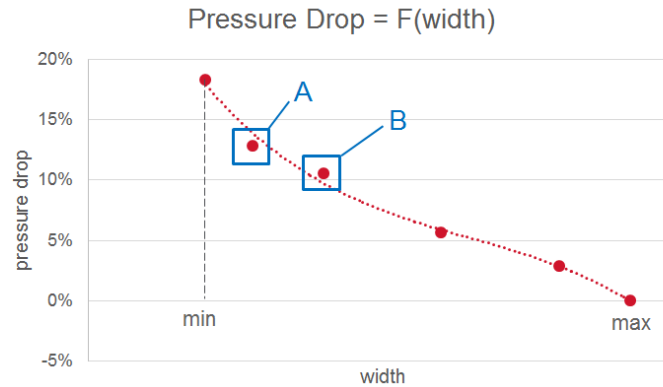
Προστίθεται και εξετάζεται άλλη μία παράμετρος σχετική με το πλάτος του αγωγού (Σχήμα 17). Από την παραμετρική μελέτη για το πλάτος προκύπτουν οι αποδόσεις των 5 νέων γεωμετριών μειωμένου πλάτους (Σχήμα 18 και Σχήμα 19).



Σχήμα 17: Παράμετρος μορφοποίησης χωρίου: Πλάτος



Σχήμα 18: Ταχύτητες για αγωγούς μειωμένου πλάτους



Σχήμα 19: Πτώση ολικής πίεσης σε αγωγούς μειωμένου πλάτους

Οι αγωγοί με τα μειωμένα πλάτη (A και B) έχουν ικανοποιητική απόδοση σε σχέση με τον αρχικό αγωγό και αποφασίζεται να εξετασθούν περαιτέρω.

Ορισμός Νέας Αντικειμενικής Συνάρτησης

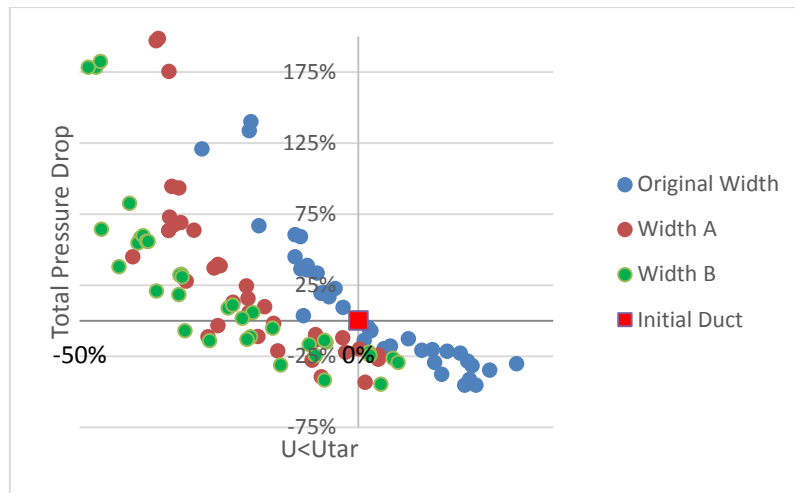
Όπως αναφέρθηκε προηγουμένως, η αντικειμενική συνάρτηση που χρησιμοποιούταν μέχρις εδώ, εκφράζει την απόκλιση των ταχυτήτων από την επιθυμητή, στο άνω τμήμα του παρμπρίζ. Καθώς πλέον στους αγωγούς που εξετάζονται οι ταχύτητες είναι υψηλότερες στο άνω τμήμα και δεν μπορεί να προβλεφθεί σε ποιες περιοχές θα παρουσιαστεί έλλειμμα ταχυτήτων, διαφαίνεται η ανάγκη για έκφραση νέα αντικειμενικής συνάρτησης που θα είναι πιο αντιπροσωπευτική του στόχου της μελέτης. Η νέα αντικειμενική συνάρτηση είναι σιγμοειδής και η μαθηματική έκφραση αυτής είναι:

$$F_{obj} = \frac{1}{\Omega_{tar}} \int_{\Omega_{tar}} 1 - \frac{1}{1 + e^{-k_2(u - u_{min}) + k_1}} d\Omega_{tar}, k_1 = \ln\left(\frac{1}{e_{inf}} - 1\right) \& k_2 = \frac{2k_1}{u_{max} - u_{min}}$$

$$f_{obj}(u) \rightarrow \begin{cases} 1 - e_{inf} \cong +1, & u \leq u_{min} \\ e_{inf} \cong +0, & u \geq u_{max} \end{cases}$$

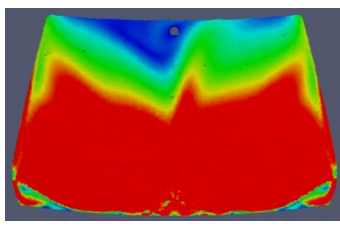
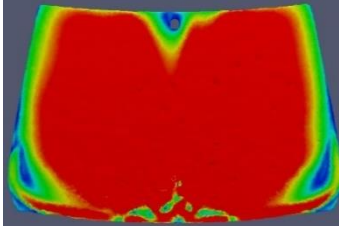
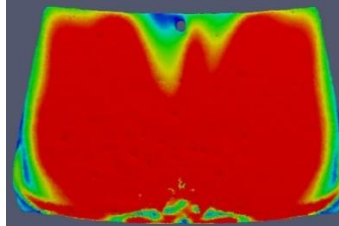
Αποτελέσματα μελέτης

Επαναλαμβάνεται η μελέτη Σχεδιασμού Πειραμάτων, και για τις δυο περιπτώσεις μειωμένου πλάτους (A και B) κατασκευάζονται: $3^3 + 2^3 = 35$ γεωμετρίες οι οποίες και αξιολογούνται με τον κώδικα CFD. Η απόδοση των 35 γεωμετριών για κάθε περίπτωση πλάτους καθώς και του αρχικού πλάτους παρουσιάζονται στο Σχήμα 20.



Σχήμα 20: Απόδοση γεωμετριών αρχικού και μειωμένου πλάτους

Αξιολογώντας τα αποτελέσματα των μελετών προκύπτει ότι και για τα δυο εξεταζόμενα πλάτη, οι πιο υποσχόμενες γεωμετρίες παίρνουν ίδιες τιμές παραμέτρων. Οι τιμές των παραμέτρων καθώς και οι τιμές της αντικειμενικής συνάρτησης και πτώσης ολικής πίεσης παρουσιάζονται Σχήμα 21.

Parameter Values	<u>Original Duct</u>	<u>Width A</u> D: Max O: Nominal A: Max	<u>Width B</u> D: Max O: Nominal A:
Performance	- -	$F_{obj} = -26.9\%$ $p_t = -11.5\%$	$F_{obj} = -26.7\%$ $p_t = -14.1\%$
Duct Performance			

Σχήμα 21: Γεωμετρία και απόδοση βέλτιστων αγωγών πλάτους A και B